NLRP3 aggravates EAE pathogenesis by modulating BBB permeability and neutrophil functionality in the mouse brain

Jaeho Lee

The Graduate School
Yonsei University
Department of Medical Science

NLRP3 aggravates EAE pathogenesis by modulating BBB permeability and neutrophil functionality in the mouse brain

A Dissertation Submitted
to the Department of Medical Science
and the Graduate School of Yonsei University
in partial fulfillment of the
requirements for the degree of
Doctor of Philosophy in Medical Science

Jaeho Lee

December 2024

This certifies that the Dissertation of Jaeho Lee is approved

Thesis Supervisor: Young-Min Hyun

Thesis Committee Member#1: Je-Wook Yu

Thesis Committee Member#2: Se Hoon Kim

Thesis Committee Member#3: Hosung Jung

Thesis Committee Member#4: Sang-Uk Seo

The Graduate School
Yonsei University

December 2024

ACKNOWLEDGEMENTS

Foremost, I cannot find words to express my gratitude to my academic advisor, Professor Young-Min Hyun, for inspiring me to do this research. Professor Hyun provided an encouraging research environment, along with his invaluable time and feedback, all of which were essential for improving my dissertation. For this, I am sincerely grateful. I would like to thank my dissertation committee members, Professor Je-Wook Yu, Professor Se Hoon Kim, Professor Hosung Jung, and Professor Sang-Uk Seo, for generously giving their time and expertise to support the completion of this dissertation.

I would like to thank all my lab mates, both past and present, for their help with my experiments. We also exchanged ideas, provided each other with feedback, and discussed challenging assignments together. This meaningful interaction inspired me to explore the information from new perspectives.

Finally, I would like to express my deepest gratitude to my family, especially Doohee Lee, Kyeonghee Lee, and Hawol Kim. Your unwavering love, support, and encouragement have been the foundation of my strength throughout this journey. Il-Geun Park, Seho Kim, and Eunsang Kwag have held me up through the lows and celebrated all the highs. I am profoundly grateful to my beloved Dr. Jiyoung Jeong for her tremendous assistance. She has brought true happiness into my life with her warm encouragement and presence. Thank you for always being there.

This dissertation would not have been possible without the love and support of all of you. I express my sincere gratitude.

TABLE OF CONTENTS

LIST OF FIGURES

LIST OF TABLES

ABSTRACT

NLRP3 aggravates EAE pathogenesis by modulating BBB permeability and neutrophil functionality in the mouse brain

Neutrophil infiltration and neutrophil extracellular traps (NETs) have been reported to be linked with several brain disorders, such as experimental autoimmune encephalomyelitis (EAE). Studies have demonstrated that NLRP3, an intracellular sensor molecule, affects neutrophil functionality and infiltration in the inflamed brain. However, the detailed molecular mechanisms underlying the NLRP3 inflammasome in these processes is largely unknown. Furthermore, the molecular pathway by which the NLRP3 inflammasome contributes to EAE progression is still elusive. The findings of this study showed that neutrophils lead to initial neuroinflammation through NLRP3 expression. While NLRP3 is dispensable for neutrophil priming, it is essential for neutrophil infiltration. Especially, NLRP3 activation in neutrophils induced CXCR2-dependent BBB disruption and neutrophil infiltration to brain through increasing CXCL1 and CXCL2 expression. Moreover, CXCL1 and CXCL2, produced by astrocytes, pericytes, neutrophils, and endothelial cells in the inflamed brain, can directly reduce Claudin-5 expression, a

junctional protein that regulates BBB permeability, in brain endothelial cells. In EAE model, the data showed that during EAE pathogenesis, neutrophils infiltrate the CNS and form NETs, leading to their accumulation. In addition, NLRP3 inflammasome promotes the generation of NET, exacerbating EAE severity by facilitating the infiltration of $CD4^+$IL-$17A^+$, $CD4^+$IFN-γ^+, and $CD4^+$IFN-γ^+IL-$17A^+$ cells to the CNS and contributing demyelination. The findings of this study indicate that the NLRP3 inflammasome regulates the migration pattern and functional phenotypes of neutrophils, enhancing their infiltration and ROS-mediated NET formation in brains. Thus, targeting the NLRP3 inflammasome could be considered a therapeutic strategy to reduce BBB disruption, neutrophil infiltration, and NET generation in the brain, thereby lessening the severity of EAE.

Key words : neutrophils, neutrophil extracellular traps (NETs), multiplesclerosis, experimental autoimmune encephalomyelitis (EAE), NLR family, pyrin domain-containing 3 protein (NLRP3), CXCR2, demyelination, blood-brain barrier

1. Introduction

Neutrophils are generally identified as the first line of defense against inflammation and the most abundant cell type in human blood[1-3]. In response to infections and injuries, neutrophils exit blood vessels and migrate into the inflamed interstitial tissue. Once neutrophils enter the interstitial tissue, they perform antimicrobial functions, including degranulation, phagocytosis, and the formation of neutrophil extracellular traps (NETs)[2]. In addition, they also produce cytokines and modulate the activities of neighboring cells[4,5]. Previous studies have shown that neutrophil infiltration is linked to various brain diseases, including traumatic brain injury[6], multiple sclerosis[7,8], ischemic stroke[9,10], and Alzheimer's disease[11,12]. Specifically, neutrophil depletion attenuates infarct volume and neurological deficits in ischemic stroke[13], improves cognitive function in Alzheimer's disease[11], and mitigates experimental autoimmune encephalomyelitis (EAE) severity[14], highlighting the potential therapeutic benefits of this intervention across various brain diseases. Considering the link between neutrophils and brain disease, it is worthwhile to investigate the factors that contribute to the process of neutrophil infiltration to the brain tissue.

During inflammation, the neutrophil infiltration generally follows a sequential multistep pathway, including tethering, rolling, adhesion, and crawling. The subsequent stage is transendothelial migration across blood-brain barrier (BBB) including the paracellular[15] or transcellular pathway[16]. The BBB limits the passage of immune cells and

plasma molecules into the brain interstitial tissue and is composed of endothelial cells (ECs) connected by junctional proteins. Previous studies have demonstrated that BBB disruption coincides with the neutrophil infiltration in the inflamed brain[17-19]. Moreover, neutrophils have been reported to increase BBB permeability, as evidenced by the findings that primed neutrophils secrete cytokines and chemokines that can directly affect BBB permeability[20,21]. However, the detailed mechanism of interplay between neutrophils and vascular damage is not yet fully understood.

NOD-like receptor family, pyrin domain-containing 3 (NLRP3) is the most extensively studied intracellular sensor molecule, recognizing a broad range of endogenous danger signals, microbial patterns, and environmental irritants, leading to the formation and activation of the NLRP3 inflammasome[22]. Previous evidence indicates that NLRP3 affects neutrophil functionality and neutrophil recruitment to inflamed tissue[23-27]. Particularly, in the bacteria infected mouse brain, the lack of NLRP3 decreased neutrophil recruitment[28]. However, the precise molecular mechanism underlying NLRP3 inflammasome in the infiltration of neutrophils into the brain is still elusive.

EAE, a mouse model for studying multiple sclerosis (MS), is an autoimmune demyelinating disease affecting the central nervous system (CNS)[29,30]. During EAE pathogenesis, activated Th1 and Th17 lymphocytes infiltrate the CNS, and these T cells are further expanded by local production of IL-1β by microglia and neutrophils. Activation of these immune cells produces nitrogen species, proteases, reactive oxygen species, and cytotoxic products, thereby contributing to demyelination[31]. Prior studies have

demonstrated the association between NLRP3 inflammasome and the pathogenesis of EAE, as evidenced by the finding that lack of NLRP3 alleviates disease severity[32-34]. Additionally, it has been indicated that infiltration of neutrophils is critical for the initiation of EAE, as supported by the findings that prophylactic anti-Ly6G treatment alleviated EAE symptoms, whereas treatment after EAE onset failed to show such effects[14]. Given that NLRP3 contributes to neutrophil functionality by promoting NET formation[23] and that serum from relapsing-remitting MS patients contains elevated levels of NET components[8], this study hypothesized that NLRP3 could regulate NET formation and thereby contribute to EAE progression.

The purpose of this study was to illuminate the unexplored elements of the mechanism associated with NLRP3, BBB disruption, and neutrophil infiltration, and their impact on the progression of EAE. Additionally, this study examines the role of the NLRP3 inflammasome in modulating NET formation within the CNS during the pathogenesis of EAE.

2. MATERIALS AND METHODS

2.1. Mice

C57BL/6N mice were obtained from Orientbio (Republic of Korea). *Ela*^{Cre} (EMMA#EM00075) mice were obtained from European Mouse Mutant Archive. *LysM*^{GFP} (MMRRC#012039) mice were obtained from Mutant Mouse Resource and Research Centers. *Nlrp3*^{D301NneoR} (JAX#017971) mice were obtained as a gift from professor Je-Wook Yu (Yonsei University, Republic of Korea). The *Nlrp3*^{D301NneoR} mice contain a neomycin cassette inserted in intron 2 of NLRP3 coding DNA, oriented oppositely to the gene, leading to the suppression of NLRP3. The mice also possess a point mutation in exon 3, resulting in a missense mutation (D301N) associated with enhanced functionality in NLRP3. To generate the neutrophil-specific expression of NLRP3 active mutant (D301N), a constitutively active form of NLRP3[35,36], *Nlrp3*^{D301NneoR} mice were crossed with *Ela*^{Cre} mouse. The *Ela*$^{Cre/+}$*;Nlrp3*$^{D301NneoR/+}$ mice have the neomycin cassette deleted in the neutrophils, allowing expression of the NLRP3 active mutant (D301N), while the other cells, Cre-negative cell population, present a NLRP3$^{-/+}$ phenotype. For visualizing neutrophils, *LysM*^{GFP} mice were crossed with *Nlrp3*^{D301NneoR} or *Ela*^{Cre}*;Nlrp3*^{D301NneoR}. Mice were subjected to intraperitoneal administration of either 0.8 mg/kg of Lipopolysaccharide (LPS) (O111:B4, Sigma-Aldrich, Germany) or phosphate buffered saline (PBS). In some experiments, Mice received 0.5 mg/kg of the CXCR2 antagonist SB225002 (Sigma-Aldrich, Germany) via intraperitoneal administration to obstruct CXCR2 signaling [37]. All

experiments were performed in line with the approved guidelines of Institutional Animal Care and Use Committee (IACUC) at Yonsei University.

2.2. Immunoblotting analysis

PRO-PREP solution (Intron Biotechnology, Republic of Korea) was applied to extract mouse whole brain proteins following a method previously described[23,24]. “Proteins were resolved by molecular weight using SDS-PAGE, after which the gels were transferred onto PVDF membranes. The membranes were subsequently blocked by incubation in a 5% non-fat milk solution (Bio-Rad, CA, USA) to prevent non-specific binding.” The following antibodies were used: “anti-mouse NLRP3 (AdipoGen Life Sciences, CA, USA), anti-mouse MPO (Abcam, MA, USA), anti-mouse CitH3 (Abcam), and anti-mouse PAD4 (Abcam) antibodies”.

2.3. Enzyme-linked immunosorbent assay (ELISA)

Mouse brain proteins were obtained using PRO-PREP, as described above. The concentrations of cytokines were measured by IL-1β ELISA kit (R&D Systems, MN, USA) in line with the manufacturer’s guidelines.

2.4. Single-cell dissociation from CNS

To isolate CNS composed cells, 9 parts of Percoll (GE Healthcare, Sweden) were mixed with 1 part of 10× Hanks' Balanced Salt Solution (HBSS) to prepare a stock solution of isotonic Percoll (SIP) solution. Spinal cords were incubated in 1 mg/mL of DNase1 (Sigma-Aldrich) and Collagenase D (Sigma-Aldrich) shaking at 80 RPM for 40 min at 37°C. Homogenized CNS tissues were seived through a 70 μm nylon mesh (SPL, Republic of Korea). The CNS cell pellets were resuspended in 30% SIP and carefully layered onto 70% SIP. The samples were then centrifuged at 500 g for 30 min. 2–3 mL of the interface between 70% and 30% was collected[24,38,39].

2.5. Flow cytometry

During the flow cytometry procedure, including antibody staining, FACS buffer composed of PBS with 2 mM EDTA and 2% FBS was used. Cell solutions were cultivated with anti-mouse CD16/CD32 (93, Biolegend, CA, USA) to prevent non-specific immunoglobulin binding to Fc receptors. For intracellular staining, cell suspensions were incubated with Cell Stimulation Cocktail solution (eBioscience, CA, USA), and then the cell mixtures were permeabilized with Fixation/Permeabilization Kit (ThermoFisher, CA, USA) in accordance with the manufacturer's directions. To discriminate between vascular and tissue leukocyte, the intravascular staining protocol was applied, as previously described[40]. "In brief, mice received an intravenous administration of 3 μg of anti-CD45 antibody. After 3 min, cold PBS was used to perfuse the mice before the brain was dissected." The brain cells were obtained according to the Single-cell dissociation protocol,

as described above. The following antibodies were used: “PerCP anti-mouse CD45 (30-F11, Biolegend), APC/cy7 anti-mouse CD45 (30-F11, Biolegend), APC anti-CD11b (M1/70, Biolegend), BV421 anti-CD11b (M1/70, Biolegend), FITC anti-mouse Ly-6G (1A8, Biolegend), PE anti-mouse Ly-6G (1A8, Biolegend), APC/Cy7 anti-mouse Ly-6G (1A8, Biolegend), Alexa Fluor 700 anti-mouse Ly-6C (HK 1.4, Biolegend), Alexa Fluor 700 anti-mouse NLRP3 (R&D Systems, MN, USA), PE anti-mouse Ly-6C (HK 1.4, Biolegend), PE anti-mouse CD18 (M18/2, Biolegend), and APC anti-mouse CD11a (M17/4, Biolegend)”. Data were obtained on an LSR Fortessa and FACSymphony A5 (BD Biosciences, NJ, USA) and analyzed using FlowJo software (FlowJo LLC, OR, USA).

2.6. Cranial window surgery for intravital imaging

The cranial window surgery was perfomed as described previously[41,42]. “In brief, mice were thoroughly anesthetized with Zoletil at a dose of 30 mg/kg. Mice were fixed in a stereotaxic frame (Live Cell Instrument, Republic of Korea) during all surgery procedures. Hair was removed from the frontal and parietal regions of the skull, and to minimize the risk of wound infection, the skin was disinfected with an ethyl alcohol solution. The procedure was conducted under aseptic conditions. Using a micro drill, a 2 mm diameter cranial window was created in the right hemisphere, positioned 2 mm lateral and 2 mm posterior to the bregma. The exposed cerebral cortex was washed with PBS, and covered with a 3 mm round cover glass (Harvard Apparatus, Quebec, Canada) using tissue glue (3M, MN, USA). A customized metal ring was fixed with dental cement (B.J.M laboratory,

Israel) on the cranial window region." The body temperature was kept at 37℃ with the aid of heating pads (Live Cell Instrument, Republic of Korea).

2.7. Two-photon intravital microscopy

The dynamics of neutrophil migration in parenchyma or blood vessel was analyzed, as described previously[41,43]. "In other to visualize blood vessel structure, 10 or 70 kDa Red-dextran (Thermo Fisher, MA, USA) was delivered via the retro-orbital sinus. Sequential 1 μm optical sections were scanned to image the post-capillary venules within the right parietal cortex of mice, using a 1× optical zoom and a 25× objective lens at a depth of 40 μm. The images were analyzed with volocity software (PerkinElmer, MA, USA)." Imaging area was excited with a laser ranging from 800 nm to 880 nm, depending on its purpose. Vascular permeability was quantified as intensity of 10 kDa Texas Red-tagged dextran observed outside the vessel surface[44,45].

2.8. Evaluation of BBB permeability using Evans blue

Mice were intraperitoneally injected with 800 μL of 1% (w/v) Evans Blue (Sigma-Aldrich, Germany), and then transcardially perfused with PBS 1 hr later, as described previously[46,47]. "Brains from the mice was dissected out, and weighed. To quantify Evans blue, brains were blended with 1 mL of PBS, and then the solution was mixed with 1 mL of trichloroacetic acid (TCA). After centrifuging the mixture at 4000 g for 30 minutes,

absorbance was measured at 620 nm using a spectrophotometer."

2.9. Immunofluorescence

Brains from mice that underwent transcardial perfusion with cold PBS were fixed in a 10% formalin solution. The fixed brains were subsequently placed in a 30% sucrose solution and allowed to sink until the tissues settled at the bottom. The tissue was embedded in OCT compound (Leica Biosystems, IL, USA), rapidly frozen in a bath of dry ice. For immunofluorescence staining, coronal slices 20 μm thick were blocked using immunostaining buffer consisting of PBS, 5% BSA, and 0.5% Triton X-100[48] to prevent non-specific antibody binding, and following primary antibodies were used overnight at 4°C: "monoclonal anti-Claudin-5 (1:50, Invitrogen, CA, USA), polyclonal anti-ZO-1 (1:50, Invitrogen), monoclonal anti-GFAP (1:100, Biolegend), polyclonal anti-NG-2 (1:100, Sigma-Aldrich), monoclonal anti-CD31 (1:100, Biolegend), monoclonal anti-CXCL1 (1:100, Invitrogen), and polyclonal anti-CXCL2 (1:100, R&D system)" . The slides were washed with PBS three times, and then were stained for 1 hr at room temperature using following secondary antibodies: "Alexa 488 anti-mouse IgG (1:300, Invitrogen), Alexa 488 anti-rabbit IgG (1:500, Abcam), Alexa 647 anti-rat IgG (1:200, Biolegend), and Alexa 647 anti-goat IgG (1:200, Invitrogen)". The images were obtained with a confocal microscope (LSM710, Carl Zeiss, Germany).

2.10. Neutrophil isolation

Bone marrow (BM) cells were isolated from the femur of C57BL/6N mice following euthanasia in a CO2 chamber. The BM cells were incubated with 2 mL of ammonium-chloride-potassium lysis buffer (Gibco, NY, USA) at 25°C for 3 min to lyse the red blood cells. Subsequently, mouse neutrophils were isolated through negative selection with a neutrophil isolation kit (Miltenyi Biotec, Bergisch Gladbach, Germany) according to the manufacturer's instructions.

2.11. RNA extraction and quantitative real-time PCR (qPCR)

Total RNA was extracted using TRIzol Reagent (Invitrogen, CA, USA) following the manufacturer's directions. "Subsequently, 2000 ng of the total RNA was reverse transcribed into cDNA using AccuPower CycleScript RT Premix (Bioneer, Republic of Korea). The expression level of mRNA for each gene was quantified using the SYBR-Green System and the QuantStudio3 system (Applied Biosystems, CA, USA) in accordance with standard protocols. All data were normalized to *Tbp* expression."

2.12. *In vitro* culture of mouse brain endothelial cell line

The bEnd.3 cells (ATCC CRL-2299) were maintained in Dulbecco's Modified Eagle Medium supplemented with 10% FBS and 1% antibiotic-antimycotic solution according to standard protocol at 37°C in the 5% CO_2 conditioned incubator.

2.13. Annexin V/DAPI staining

To assess cell viability, cells were incubated with FITC annexin V and 1 μg/mL of DAPI solution for 15 min in the dark at 25°C. The stained cells were subsequently diluted in Annexin V-binding buffer (Biolegend), and the resulting cell suspension was analyzed by flow cytometry.

2.14. EAE induction

EAE induction was performed using the MOG_{35-55}/CFA Emulsion PTX kit (Hooke Labs, MA, USA) in accordance with the protocol provided by the manufacturer. "Ten- to twelve-week-old female C57BL/6N, $Ela^{Cre/+}$, or $Ela^{Cre/+};Nlrp3^{D301NneoR/+}$ mice were immunized subcutaneously at two sites on their back with MOG_{35-55} emulsified in complete Freund's adjuvant (CFA). Following this, pertussis toxin (PTX) was administered intraperitoneally twice, at 2 and 24 hr after the initial immunization. EAE-induced mice were then randomly assigned to different treatment groups. Clinical scores for EAE were assessed daily in a blinded manner by two independent observers, using the following scale: 0 indicates no apparent signs of disease; 0.5 signifies a partially limp tail; 1 represents a completely limp tail; 1.5 denotes a limp tail with waddling gait; 2 indicates a limp tail and complete paralysis of one hind limb; 2.5 corresponds to a limp tail, complete paralysis of one hind limb, and partial paralysis of the other; 3 indicates a limp tail and complete paralysis of both hind limbs; 3.5 signifies a limp tail, complete paralysis of both hind limbs, and ascending paralysis; 4 represents trunk paralysis; 4.5 indicates moribund status; and 5 denotes death"[49,50].

2.15. Elimination of NETs *in vivo*

To remove the accumulated NETs, mice received simultaneous injections of 10 μg of human recombinant DNase1 (ProSpec, Israel) intravenously and 50 μg intraperitoneally[51,52], starting from day 7 post-immunization. Following this initial dose, an additional 50 μg was administered intraperitoneally every 24 hr.

2.16. Luxol fast blue staining

To quantify demyelination area in CNS of mice, fixed tissue samples were stained with the Luxol Fast Blue Stain Kit (Abcam), following the manufacturer's instructions. "The tissue sections were incubated in 0.1% Luxol fast blue solution for 2 hr at 24°C and subsequently differentiated in 0.05% lithium carbonate solution. Upon completion of the differentiation process, the sections were counterstained with 0.1% cresyl echt violet solution for 3 min at 24°C. The analysis of demyelination was performed in the corpus callosum region of the brain and the thoracic to lumbar regions of the spinal cord. The extent of demyelination in the white matter was quantified using ImageJ software (NIH, USA)"[34,53].

2.17. Imaging data analysis

Volocity (PerkinElmer, MA, USA), Imaris (Bitplane, Switzerland), and Fiji/Image

J (NIH, MD, USA) were used for imaging data analysis.

2.18. Statistical analysis

Statistical analysis was conducted using Prism v9.0 (GraphPad, CA, USA). To compare two or more samples, either a Student's t-test or one-way ANOVA was performed. For grouped samples, two-way ANOVA was employed. For EAE disease data, a log-rank test using Mantal-Cox method was conducted. A P-value of less than 0.05 was regarded as statistically significant. *P<0.05, **P<0.01, ***P<0.001, ****P<0.0001.

Table 1. Primer sequences for quantifying mRNA expression

Gene symbol	"Sequence (5'-3')"
Tbp	F: "GAG TTG CTT GCT CTG TGC TG"
	R: "CTG GCT TGT GTG GGA AAG AT"
Cxcl1	F: "GCT GGG ATT CAC CTC AAG AA"
	R: "TGG GGA CAC CTT TTA GCA TC"
Cxcl2	F: "TGG AAG GAG TGT GCA TGT TC"
	R: "CAA GAC ACG AAA AGG CAT GA"
Mmp2	F: "CCC CTG ATG TCC AGC AAG TAG A"
	R: "AGT CTG CGA TGA GCT TAG GGA AA"
Mmp9	F: "CCC TGG AAC TCA CAC GAC ATC TTC"
	R: "GGT CCA CCT TGT TCA CCT CAT TTT"
Hmox1	F: "TCC GCA TAC AAC CAG TGA GT"
	R: "CAG GGC CGT GTA GAT ATG GT"
Pad4	F: "GGC TAC ACA ACC TTC GGC AT"
	R: "GCT GCT TTC ACC TGT AGG GT"

3. RESULTS

PART I. NLRP3 activation in neutrophils accelerates onset, and increases score and incidence of EAE via CXCR2-dependent BBB disruption and neutrophil infiltration in the mouse brain

3.1. NLRP3 inflammasome promotes the neutrophil infiltration to inflamed brain tissue

To markedly activate NLRP3 expression in brain, mice were injected with LPS (0.8 mg/kg/day) at 24 hr intervals for 2 days (Figure 1A) as described previously[41,54]. After 48 hr post-first LPS injection, we confirmed that NLRP3 expression and IL-1β production were significantly increased in the brain of LPS group compared to the PBS group (Figure 1B and C). Interstitial leukocytes situated within tissue layers can be mixed with circulating leukocytes found within the vascular system during the cell preparation process[55]. To differentiate interstitial leukocytes from circulating ones, we employed a technique involving the intravenous administration of fluorochrome-conjugated anti-mouse CD45 mAb, enabling selective staining and identification of circulating leukocytes in contrast to interstitial leukocytes[40] (Figure 2).

To investigate the impact of NLRP3 inflammasome activation on neutrophil infiltration into brain tissue, we quantified interstitial neutrophils in the brains of WT and *Nlrp3*$^{-/-}$ mice after PBS or LPS injections. Our findings showed that LPS-induced

inflammasome activation significantly elevated the number of interstitial neutrophils, an increase that was entirely absent in *Nlrp3*$^{-/-}$ mice (Figure 1D). To visualize and further corroborate the NLRP3-dependent neutrophil infiltration to brain, we conducted intravital imaging using *LysM*$^{GFP/+}$ mice that were either WT for *Nlrp3* or *Nlrp3*$^{-/-}$, as described previously[41,42]. Infiltrated neutrophils were identified by analyzing GFP^{+} cells found outside the bloodstream. Consistent with previously observed data, the number of infiltrated GFP^{+} neutrophils was increased in LPS-*LysM*$^{GFP/+}$ group compared to PBS-*LysM*$^{GFP/+}$ group (Figure 1E). However, in *Nlrp3*$^{-/-}$;*LysM*$^{GFP/+}$ mice, the infiltrated neutrophils were scarcely discernible in inflamed brain (Figure 1E). Based on the results, we found that NLRP3 activation in the brain induces neutrophil infiltration to inflamed brain tissue.

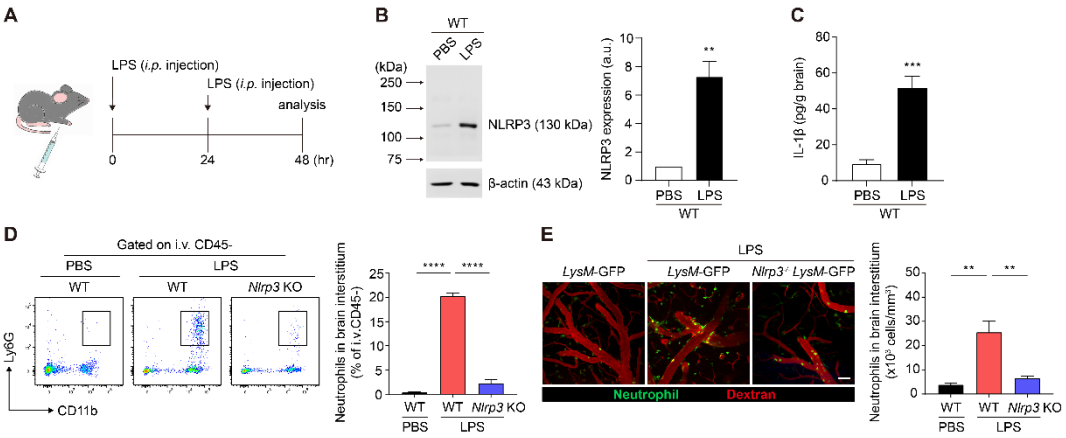

Figure 1. NLRP3 deficiency attenuates the neutrophil infiltration to inflamed brain tissue. (A) Experimental scheme for LPS injection to induce neuroinflammation. (B) Immunoblotting and densitometric analysis for NLRP3 expression in the brain. (C) ELISA analysis for IL-1β in the brain. (D) Scatter plots of brain interstitial leukocytes and percentage value of neutrophils. *i.v.* CD45: intravenously injected anti-mouse CD45 antibody. (E) Representative intravital images and the density of interstitial neutrophils in brains. Green: Neutrophils, Red: Texas Red-dextran. Scale bar, 50 μm. Mean values are shown with the SEM. The data were derived from a minimum of three independently conducted experimental replicates.

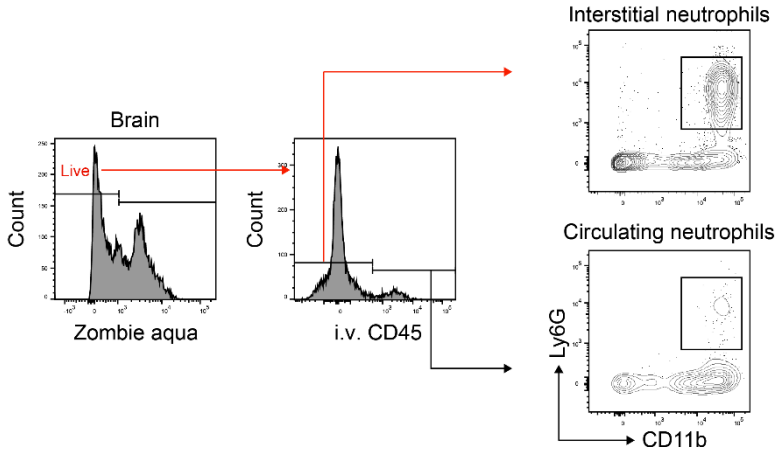

Figure 2. Gating strategy to discriminate interstitial neutrophils from circulating neutrophils via flow cytometry. First, the population of negative signal for Zombie Aqua dye was gated to identify live cell population. The population of negative signal for *i.v.* CD45 (intravenously injected Anti-mouse CD45 antibody) was gated to distinguish interstitial leukocytes from circulating leukocytes. $CD11b^{+}$ $Ly6G^{+}$ cells were classified as interstitial or circulating neutrophils depending on whether they were negative or positive for *i.v.* CD45, respectively.

3.2. NLRP3 inflammasome facilitates the neutrophil intravasation from bone marrow to blood vessels

Neutrophils complete several developmental stages to reach maturity in the bone marrow before being released into peripheral blood, where they perform surveillance functions[2,56]. We next explored the potential role of the NLRP3 inflammasome in regulating the movement of neutrophils from the bone marrow into peripheral blood. The LPS-*Nlrp3*$^{-/-}$ group showed an increase in BM neutrophils and a decrease in blood neutrophils compared to LPS-WT group, suggesting that NLRP3 inflammasome facilitates the neutrophil intravasation from BM to peripheral blood (Figure 3A and B). Taken together, NLRP3 inflammasome promotes the neutrophil intravasation from bone marrow.

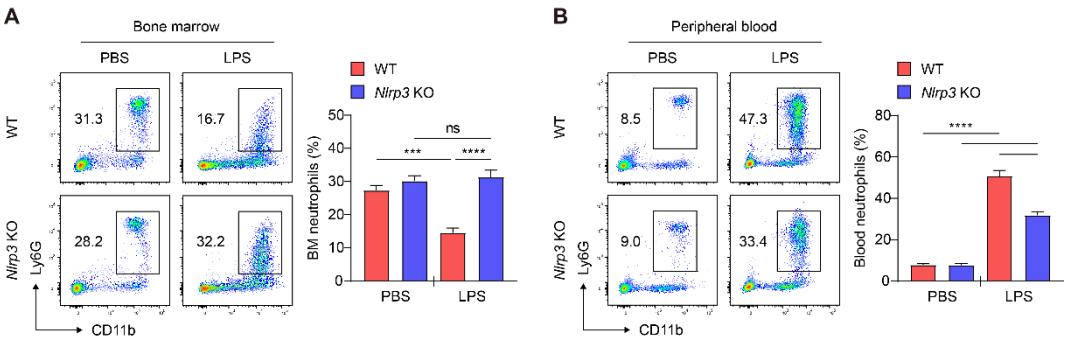

Figure 3. NLRP3 inflammasome promotes the neutrophil intravasation from BM to peripheral blood. Scatter plots of (A) bone marrow or (B) blood neutrophils and percentage value of these cells were presented. The data were derived from a minimum of three independently conducted experimental replicates. Mean values are shown with error bars representing the SEM.

3.3. NLRP3 inflammasome induces BBB disintegration

Recent evidence demonstrates that the neutrophil infiltration to inflamed brain is associated with blood-brain barrier (BBB) disintegration[19,57]. The BBB consists of a tightly packed endothelial cell (EC) monolayer brought together by junctional proteins such as Claudin-5 and ZO-1[58]. To measure the BBB integrity *in vivo*, we examined the expression level of junctional proteins in sectioned brain tissue. In the PBS injection group, pronounced expression of Claudin-5 and ZO-1 was observed in both WT and *Nlrp3*$^{-/-}$ mice. However, following LPS injection, WT mice showed diminished expression of Claudin-5 and ZO-1, whereas *Nlrp3*$^{-/-}$ mice exhibited a notable expression of these proteins (Figure 4A and B). The results indicate that NLRP3 inflammasome promotes BBB disruption.

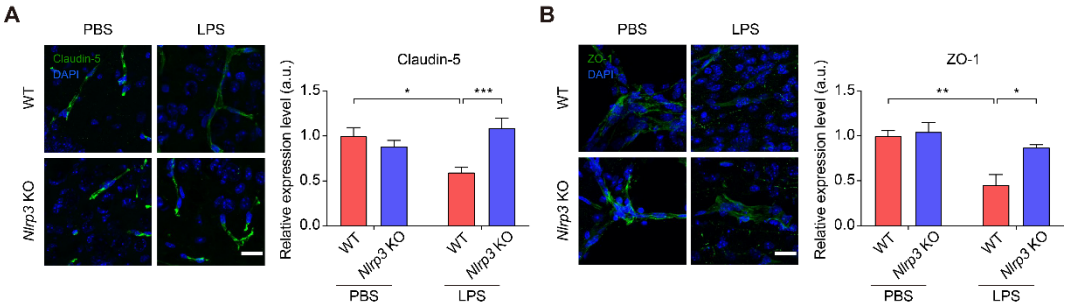

Figure 4. NLRP3 inflammasome reduces BBB integrity. In the brain tissue, representative fluorescent images and graph of (A) Claudin-5 and (B) ZO-1 were presented. Fluorescence images were obtained, following the staining for junctional proteins (green) and nuclei (blue). Scale bar, 50 μm. a.u., arbitrary unit. Mean values are shown with error bars representing the SEM.

3.4. Neutrophils mainly contribute to initial neuroinflammation through NLRP3 expression

Next, to determine the primary cell types contributing to triggering the NLRP3 dependent neuroinflammation, we assessed the NLRP3 expression levels and cellular activity in different immune cell types from brain tissue at the early stages of LPS-induced neuroinflammation. At 1 or 3 hr post-LPS injection in WT mice, we measured the expression levels of NLRP3 and CD11b in neutrophils, monocytes, and microglia by flow cytometry. To define these immune cell population, we initially gated live singlets, isolated $CD11b^{+}$ $Ly6G^{+}$ neutrophils, and then isolated $CD45^{lo/int}$ $CD11b^{+}$ microglia from the $CD11b^{+}$ $Ly6G^{-}$ population. Subsequently, among the $CD45^{hi}$ $CD11b^{+}$ population, we further gated $Ly6C^{hi}$ and $Ly6C^{low}$ subsets, in accordance with a previously reported[59] (Figure 5). CD11b has been associated with a primed phenotype in the aforementioned immune cell types[24,60-62]. The data showed that WT neutrophils exhibited an elevation in the expression levels of NLRP3 and CD11b at 3 h post-LPS injection compared to the control (Figure 6A and B). In contrast, the expression levels of these molecules showed no significant differences in WT $Ly6C^{hi}$, $Ly6C^{low}$, and microglia (Figure 7A and B). These data reveal that neutrophils may contribute to initial neuroinflammation through elevating NLRP3 expression, acting as the first responders to LPS.

In *Nlrp3*$^{-/-}$ mice, NLRP3 was not detected in neutrophils (Figure 6A). Interestingly, neutrophils in *Nlrp3*$^{-/-}$ mice exhibited an elevation in the expression levels of CD11b at 3 h post-LPS injection, suggesting that NLRP3 was unnecessary for neutrophil priming (Figure

6B). As shown in figure 1D and E, however, neutrophils in *Nlrp3*$^{-/-}$ mice failed to infiltrate to inflamed brain. These data demonstrate that NLRP3 is dispensable for neutrophil priming but required for the neutrophil infiltration to brain. Taken together, our findings reinforce the necessity of further investigating the effect of NLRP3 in neutrophils on the neuroinflammation including neutrophil infiltration and BBB disintegration.

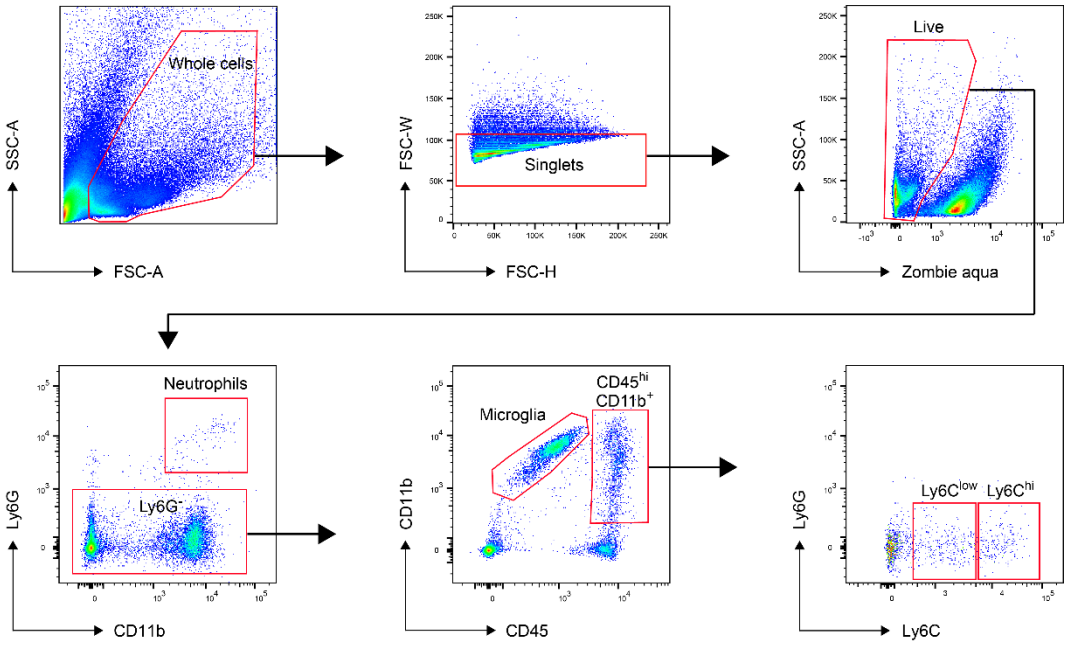

Figure 5. Gating strategy to define neutrophils, monocytes, and microglia population. Singlets were gated to avoid the unexpected false positive signal for fluorescence labeled antibody. First, the population of negative signal for Zombie Aqua dye was gated to identify live cell population. Within the live cells, the $CD11b^{+}$ $Ly6G^{+}$ population was denoted as neutrophils, and $CD45^{lo/int}$ $CD11b^{+}$ microglia were isolated from the $CD11b^{+}$ $Ly6G^{-}$ population. Subsequently, within the $CD45^{hi}$ $CD11b^{+}$ population, we further gated $Ly6C^{hi}$ and $Ly6C^{low}$ subsets.

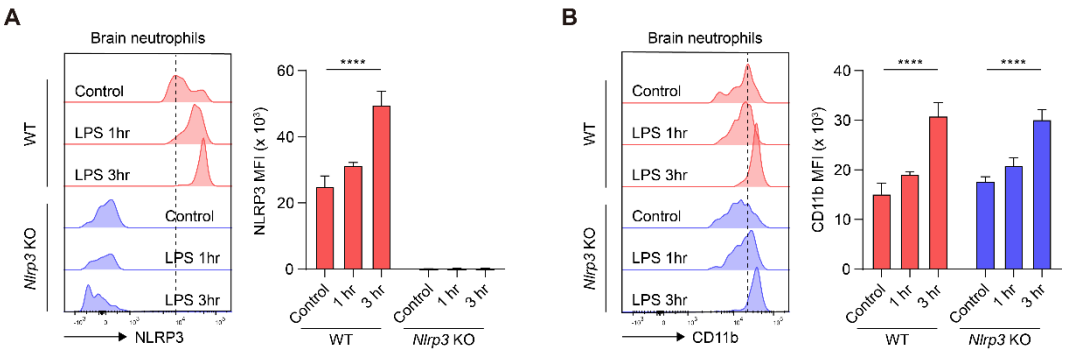

Figure 6. Neutrophils contribute to initial neuroinflammation through NLRP3 expression, but NLRP3 is dispensable for neutrophil priming. (A and B) Representative histogram and mean fluorescence intensity (MFI) of the NLRP3 and CD11b expression of neutrophils in the brain. The dotted line defines the histogram peak in the control group of WT mice. The data were derived from a minimum of three independently conducted experimental replicates. Mean values are shown with error bars representing the SEM.

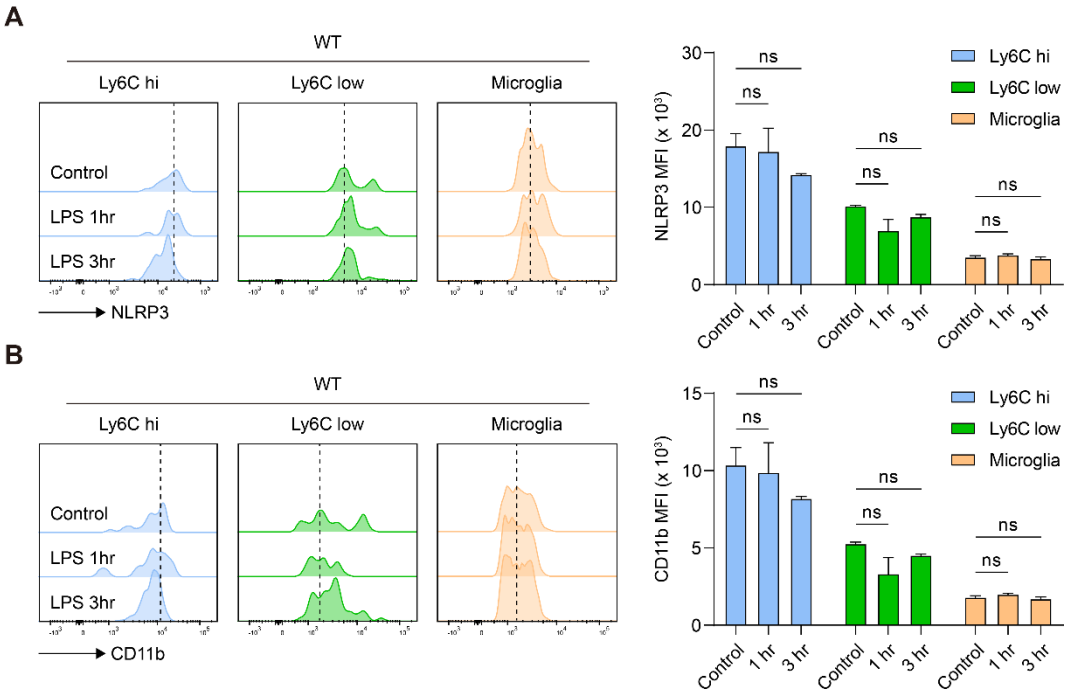

Figure 7. At initial neuroinflammation, WT Ly6C^{hi}, Ly6C^{low}, and Microglia exhibit no notable alterations in CD11b and NLRP3 expression levels. (A and B) Representative histogram and mean fluorescence intensity (MFI) of the (A) NLRP3 and (B) CD11b expression of WT Ly6C^{hi}, Ly6C^{low}, and microglia in the brain. The dotted line defines the histogram peak in the control group of WT mice. The data were derived from a minimum of three independently conducted experimental replicates. Mean values are shown with error bars representing the SEM. ns: non-significant.

3.5. NLRP3 activation in neutrophils facilitates the neutrophil infiltration and the BBB disruption

Given that neutrophils potentially contribute to triggering neuroinflammation through NLRP3 expression, we further determine how NLRP3 in neutrophils affects neutrophil infiltration to the brain tissue and BBB integrity. We used the mice model of NLRP3 active mutant (D301N), a constitutively active form of NLRP3[35,36]. To generate a neutrophil-specific expression of NLRP3 active mutat (D301N), the active mutant mice were bred with Ela-Cre mice. Ela-Cre caused deletion of floxed neomycin cassette in neutrophils of $Ela^{cre/+}$; $Nlrp3^{D301N/+}$ mice, leading to expression of NLRP3 (D301N) in neutrophils but not in other cells (Figure 8A and B).

In the PBS injection group, control mice exhibited minimal presence of infiltrated neutrophils, while active mutant mice displayed a conspicuous increase in the number of infiltrated neutrophils within brain tissue (Figure 9A). Following LPS injection, active mutant mice showed a greater number of infiltrated neutrophils compared to control mice, indicating that NLRP3 activation in neutrophils facilitates the neutrophil infiltration (Figure 9A). Here, we focused on an increase in infiltrated neutrophils induced by neutrophil-specific NLRP3 active mutation, in accordance with previous studies[36,63]. Considering the relationship between the neutrophil infiltration and BBB disintegration as described above, our subsequent investigation aimed to identify whether NLRP3 activation in neutrophils induces BBB disruption. To examine the BBB disruption *in vivo*, we investigated the expression levels of junctional proteins in sectioned brain tissue. The active

mutant mice showed a decreased expression of Claudin-5 and ZO-1 in sectioned brain tissue (Figure 9B). Additionally, to determine whether NLRP3 activation in neutrophils affects vascular permeability in the brain, we performed intravital imaging using 10 kDa Texas Red-tagged dextran, as previously described[44,45]. Vascular permeability was quantified as intensity of 10 kDa dextran observed outside the vessel surface[44,45]. The active mutant mice showed a marked dextran leakage into the interstitium, indicating an increase in vascular permeability (Figure 9C). To further corroborate the effect of NLRP3 activation in neutrophils on vascular permeability, we evaluated BBB permeability using Evans blue, as previously described[46,47]. As described above, the NLRP3 activation in neutrophils increases vascular permeability (Figure 9D). Based on the results, we found that NLRP3 activation in neutrophils facilitates the neutrophil infiltration and BBB disintegration, and increases vascular permeability.

A

	Genotype	NLRP3 expression	
		Neutrophils	Other cells
Control (*Nlrp3* $^{+/+}$)	*Ela*$^{cre/+}$ *Nlrp3*$^{+/+}$	WT/WT	WT/WT
Active mutant (*Nlrp3* $^{D301N/+}$)	*Ela*$^{cre/+}$ *Nlrp3*$^{D301N/+}$	**D301N**/WT	–/WT

B

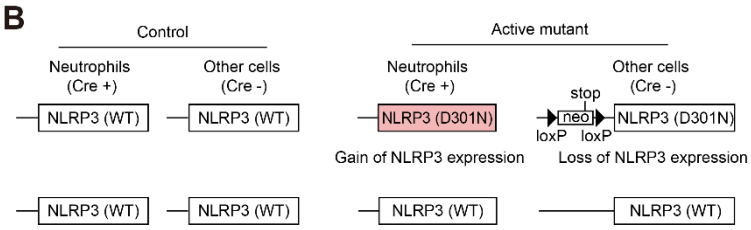

Figure 8. Generation of NLRP3 active mutant mice with conditional expression of the mutation in neutrophils. (A) Overview of genotype and Nlrp3 gene expression profiles across neutrophils and other cell types in mice. (B) Illustrative schematic representation of NLRP3 expression pattern and neomycin cassette in neutrophils and other cell types of both mice.

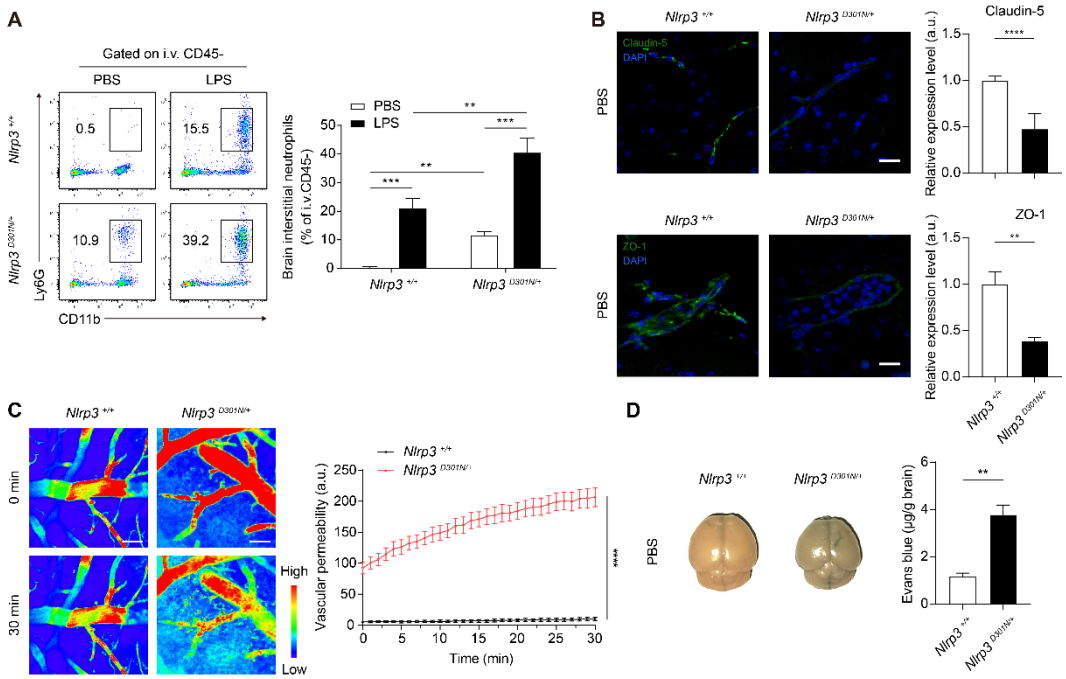

Figure 9. NLRP3 activation in neutrophils facilitates the neutrophil infiltration, and increases the vascular permeability by reducing BBB integrity. (A) Scatter plots of brain interstitial leukocytes and percentage value of neutrophils. *i.v.* CD45: intravenously injected anti-mouse CD45 antibody. (B) In the brain tissue, representative fluorescent images and graph of Claudin-5 (top panels) or ZO-1 (bottom panels) were presented. Scale bar: 50 μm. Fluorescence images were obtained, following the staining for junctional proteins (green) and nuclei (blue). a.u.: arbitrary unit. (C) Intravital imaging of brain blood vessels was performed with *i.v.* injection of 10 kDa Texas Red-dextran. A rainbow intensity scale was used to denote 10 kDa dextran leakage. Representative two-photon intravital images and graph of vascular leakage (extravascular dextran) at 0 min (top panels) and 30 min (bottom panels). Vascular leakage was quantified by calculating the intensity of

dextran outside the venules every 1 min. (D) Representative images of brain tissue and quantitative analysis of Evans blue dye accumulation within the brain. Mean values are shown with error bars representing the SEM.

3.6. CXCL1 and CXCL2 reduce extracellular Claudin-5 on brain endothelial cells

Next, we determined the potential mediator between NLRP3 activation in neutrophils and BBB disruption. Initially, mRNA expression level of CXCL1, CXCL2, MMP2, and MMP9 was measured, which is associated with BBB disruption[19,64,65]. We investigated whether NLRP3 activation in neutrophils altered the production of these proteins. Isolated neutrophils from NLRP3 active mutant mice exhibited increased CXCL1 and CXCL2 production. However, there were no notable differences in the production of MMP2 and MMP9 (Figure 10A). Based on the previous reports suggesting that BBB disruption is linked with impaired endothelium and decreased expression of tight junction[66,67], we explored whether these chemokines modulate the phenotype of brain ECs. Flow cytometry analysis was conducted to evaluate cellular damage or tight junction expression in bEnd.3 cells, which are primary mouse brain ECs[68,69]. Neither CXCL1 nor CXCL2 induced cell death or early apoptosis in brain ECs (Figure 10B). Interestingly, these chemokines significantly decreased extracellular Claudin-5 expression, but did not affect ZO-1 expression in brain ECs (Figure 10C). Taken together, these findings demonstrate that CXCL1 and CXCL2 generated due to NLRP3 activation in neutrophils can reduce the extracellular Claudin-5 expression on the brain ECs, potentially diminishing BBB integrity.

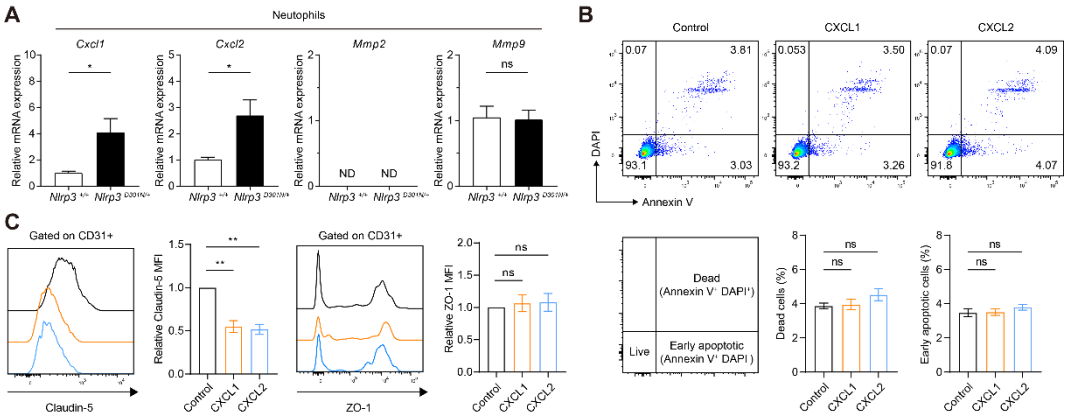

Figure 10. CXCL1 and CXCL2, which can be expressed by NLRP3-activated neutrophils, reduce extracellular Claudin-5 on brain endothelial cells. (A) Total RNA was isolated from neutrophils in the bone marrow, and the expression levels of *Cxcl1*, *Cxcl2*, *Mmp2*, and *Mmp9* were analyzed by qPCR. ND: not detectable. (B) Representative scatter plots (upper panels) and the percentage value (lower panels) of dead cells and early apoptotic cells in the brain endothelial cells. (C) Representative scatter plots and mean fluorescence intensity (MFI) of Claudin-5 (left) or ZO-1 (right) in brain endothelial cells. The data were derived from a minimum of three independently conducted experimental replicates. Mean values are shown with error bars representing the SEM. ns: non-significant.

3.7. CXCL1 and CXCL2 are produced by astrocytes, pericytes, neutrophils, and endothelial cells

We next examined which cell populations were associated with the production of CXCL1 and CXCL2. Whole-brain tissue was prepared 48 hr after the first LPS injection for confocal microscopy. Because astrocytes, pericytes, and endothelial cells form an integral components of the BBB, and neutrophils from NLRP3 active mutant mice showed increased CXCL1 and CXCL2 production, the brain sections were stained with GFAP to mark astrocytes[19], NG2 to mark pericytes[70,71] and CD31 to mark endothelial cells[71]. The brain sections of LysM-GFP mice were used to identify neutrophils[19]. CXCL1 and CXCL2 expression co-localize with $GFAP^+$ astrocytes, $NG2^+$ pericytes, $LysM^+$ neutrophils, and $CD31^+$ endothelial cells (Figure 11 and 12). These data indicate that during neuroinflammation, CXCL1 and CXCL2 are produced by astrocytes, pericytes, neutrophils, and endothelial cells.

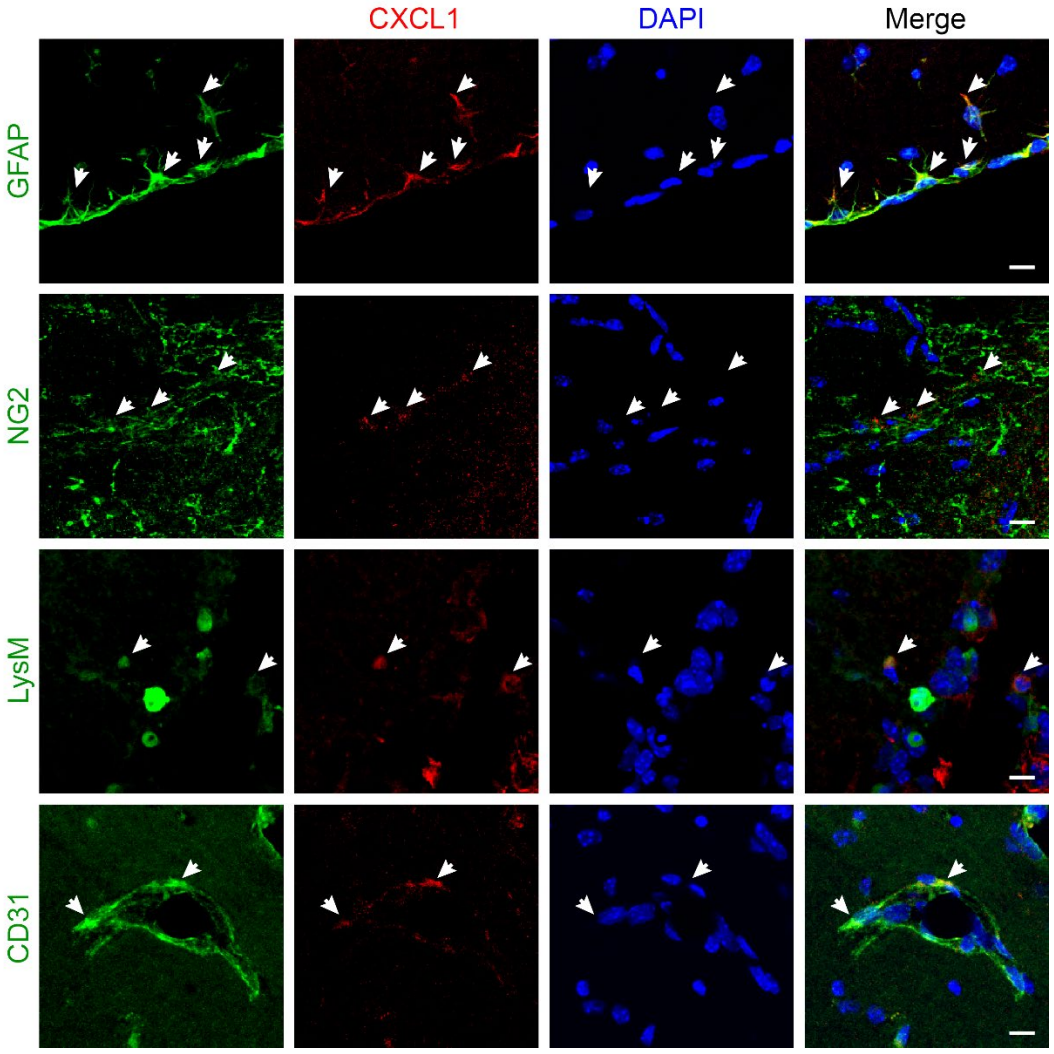

Figure 11. CXCL1 is produced by astrocytes, pericytes, neutrophils and endothelial cells. Representative fluorescent images of CXCL1 in astrocytes, pericytes, neutrophils, and endothelial cells in the brain. GFAP, NG2, LysM, and CD31 (green) denote astrocytes, pericytes, neutrophils and endothelial cells, respectively. CXCL1 (red) and nuclei (blue). Data were represented from at least four independent experiments. Scale bar: 10 μm.

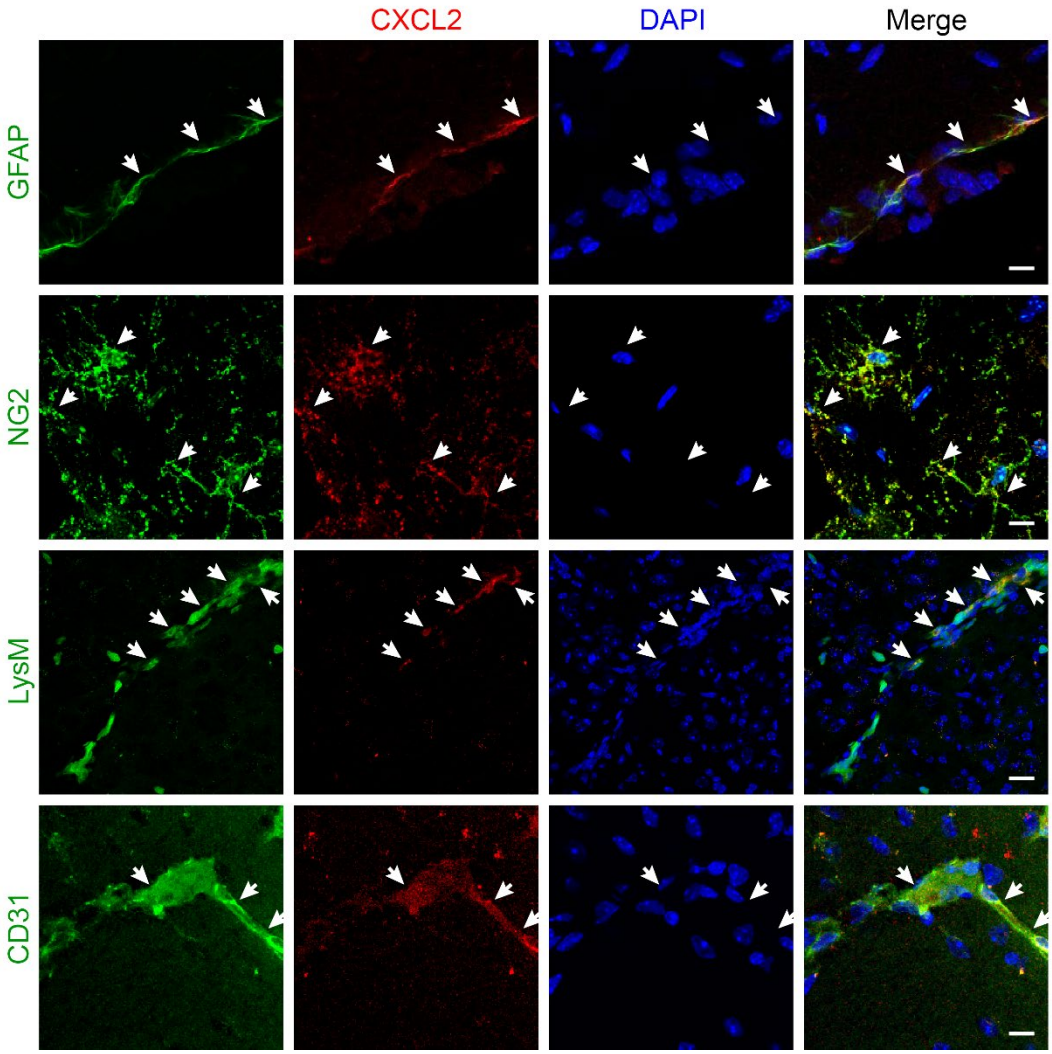

Figure 12. CXCL2 is produced by astrocytes, pericytes, neutrophils and endothelial cells. Representative fluorescent images of CXCL2 in astrocytes, pericytes, neutrophils, and endothelial cells in the brain. GFAP, NG2, LysM, and CD31 (green) denote astrocytes, pericytes, neutrophils and endothelial cells, respectively. CXCL2 (red) and nuclei (blue). Data were represented from at least four independent experiments. Scale bar: 10 μm.

3.8. CXCR2 is required for the neutrophil infiltration and the regulation of vascular permeability in the inflamed brain

To assess the impact of distinct chemokine signaling pathways on neutrophil infiltration, we studied mice in which the cognate receptors for CXCL1 and CXCL2 were blocked using selective CXCR2 antagonist. WT mice were administered an intraperitoneal injection of the antagonist 0.5 hr before LPS treatment for 2 days, while NLRP3 active mutant mice received intraperitoneal injections of the antagonist at 24 h intervals for 7 days[37,72]. We found that the blockade of CXCR2 reduced the number of interstitial neutrophils in brains of neuroinflammation models driven by LPS or NLRP3 activation (Figure 13A and B). These data indicate that CXCR2 plays a crucial role in facilitating the neutrophil infiltration to inflamed brain. Our subsequent investigation aimed to illuminate the effect of the CXCR2 signaling pathways on BBB permeability in neuroinflammation. In the neuroinflammation models induced by LPS or NLRP3 activation, the blockade of CXCR2 alleviates BBB disruption in the inflamed brain. (Figure 13C and D). Based on the results, CXCR2 is essential for the neutrophil infiltration and the BBB disruption during neuroinflammation.

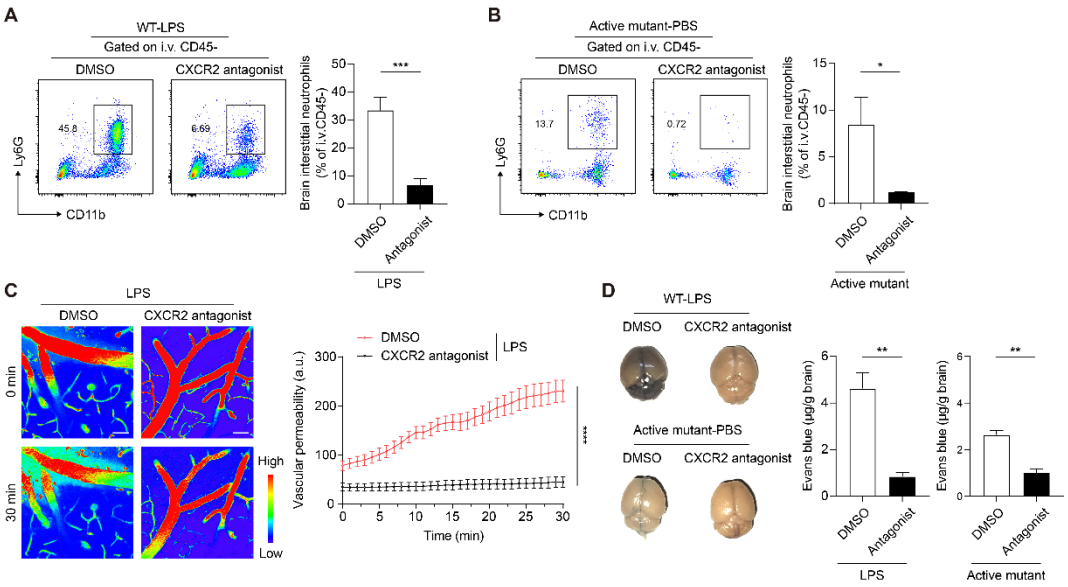

Figure 13. The blockade of CXCR2 attenuates the neutrophil infiltration and the increased vascular permeability. (A and B) Scatter plots of brain interstitial leukocytes and percentage value of neutrophils of the neuroinflammation models induced by (A) LPS or by (B) NLRP3 activation in neutrophils. *i.v.* CD45: intravenously injected anti-mouse CD45 antibody. (C) Intravital imaging of blood vessels in mice brain was performed with *i.v.* injection of 10 kDa Texas Red-dextran. A rainbow intensity scale was used to denote 10 kDa dextran leakage. Representative two-photon intravital images and graph of vascular leakage (extravascular dextran) at 0 min (top panels) and 30 min (bottom panels). Vascular leakage was quantified by calculating the intensity of dextran outside the venules every 1 min. (D) Representative images of brain tissue and quantitative analysis of Evans blue dye accumulation within the brain of the neuroinflammation models induced by LPS (top panels) or by NLRP3 activation in neutrophils (bottom panels). The data were derived from

a minimum of three independently conducted experimental replicates. Mean values are shown with error bars representing the SEM.

3.9. NLRP3 activation in neutrophils exacerbates EAE severity

Finally, we tested our hypothesis that CXCR2-mediated neutrophil infiltration and BBB disruption exacerbate the severity of brain disease. Given that neutrophil infiltration is crucial for the initiation of EAE[14], we used the EAE model, a mouse model for studying multiple sclerosis (MS), to determine whether the CXCR2-mediated neuroinflammtion, induced by NLRP3 activation in neutrophils, contributes to EAE progression. CXCR2 antagonist or vehicle were administered daily starting from day 7 before immunization with MOG_{35-55} peptide antigen (Figure 14A). The active mutant accelerated the onset and increased both clinical score and incidence of EAE compared to WT, but these effects were abolished by the CXCR2 antagonist (Figure 14B and C), suggesting that CXCR2-mediated neutrophil infiltration and BBB disruption exacerbate EAE severity.

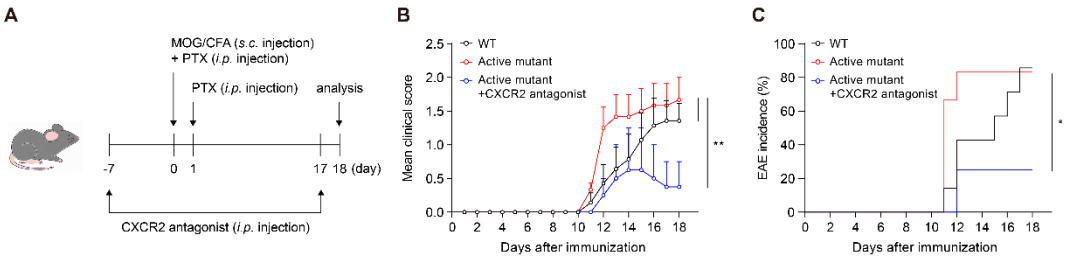

Figure 14. Active mutant increased both clinical score and incidence of EAE, and accelerated the disease onset via CXCR2-mediated neutrophil infiltration and BBB disruption. (A) Experimental scheme of EAE development. CXCR2 antagonist or vehicle were administered daily starting from day 7 before immunization with MOG_{35-55} peptide antigen. (B) Mean clinical score and (C) EAE incidence. Mean values are shown with error bars representing the SEM.

PART II. NLRP3 inflammasome exacerbates EAE severity via ROS-mediated NET formation in the mouse brain

3.10. EAE induces neutrophil infiltration and NET formation in the CNS

Initially, we evaluated the number of neutrophils that had infiltrated the CNS in mice induced with EAE to identify the essential role of neutrophils in EAE pathogenesis. Although they are considered important initial responders and have a short lifespan, a significant number of neutrophils were detected in the CNS between 17 to 19 days after immunization, coinciding with the peak of the disease. (Figure 15A and B). Neutrophils play diverse roles in the pathogenesis of MS. Among their versatile effects, this study highlights the potentially harmful impact of NET formation[73]. NETs accumulate in lesions and have been identified as a contributing factor in the development of autoimmune diseases, such as rheumatoid arthritis and experimental lupus[74,75]. Furthermore, clinical data indicate that patients with relapsing-remitting MS display circulating NET components in their serum[76]. Therefore, the levels of formed NETs in the CNS of EAE-induced mice were assessed. Citrullinated histone H3 (CitH3), a marker of NETs, was employed, as it is formed during the NET formation process when arginine residues in histones are converted into citrulline[77,78]. Additionally, MPO was utilized as a marker for NETs. It is an intracellular enzyme found in immune cells and is released as part of the NET structure[79]. Significantly, both MPO and CitH3 showed elevated expression in the

CNS of the EAE-induced mice at the peak stage of the disease (Figure 15C and D). The degree of NET formation was assessed by measuring the proportion of neutrophils that were double-positive for MPO and CitH3[80]. In brief, to identify NET-producing neutrophils, $Ly6G^+$ neutrophils were first gated from the inflamed CNS leukocyte population, followed by gating for CitH3-positive cells. MPO-positive cells were then gated within the CitH3-positive population, indicating co-expression of Ly6G, CitH3, and MPO, in accordance with prior descriptions[80] (Figure 16). These findings align with the protein expression analysis, demonstrating that EAE progression is associated with NETs in the CNS (Figure 15E and F). Notably, the results indicate that EAE leads to neutrophil infiltration and subsequent NET accumulation within the CNS, highlighting the pivotal role of neutrophils in EAE progression. This underscores the necessity of advancing research on neutrophil-targeted approaches for treating EAE.

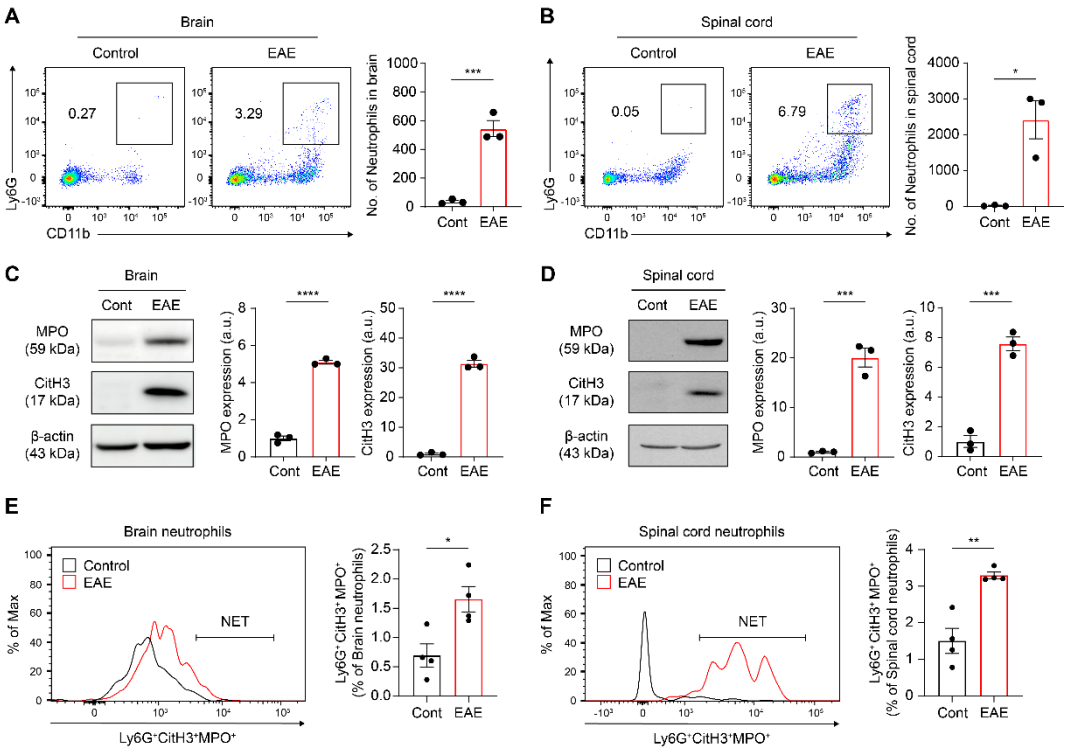

Figure 15. Significant neutrophil presence and extracellular trap formation were detected in CNS of EAE model. Assessment of the absolute number of infiltrated neutrophils and formed NETs in CNS of EAE model. Scatter plots of brain leukocytes and the absolute number of neutrophils in (A) brains or (B) spinal cord were shown. Cont. denotes non-induced EAE mice. Immunoblotting and quantification of NET components, including MPO and CitH3 in (C) brains or (D) spinal cord were presented. Histograms showing the formed NETs and percentage value in neutrophils of (E) brains or (F) spinal cord were presented. Data were presented with mean ± SEM.

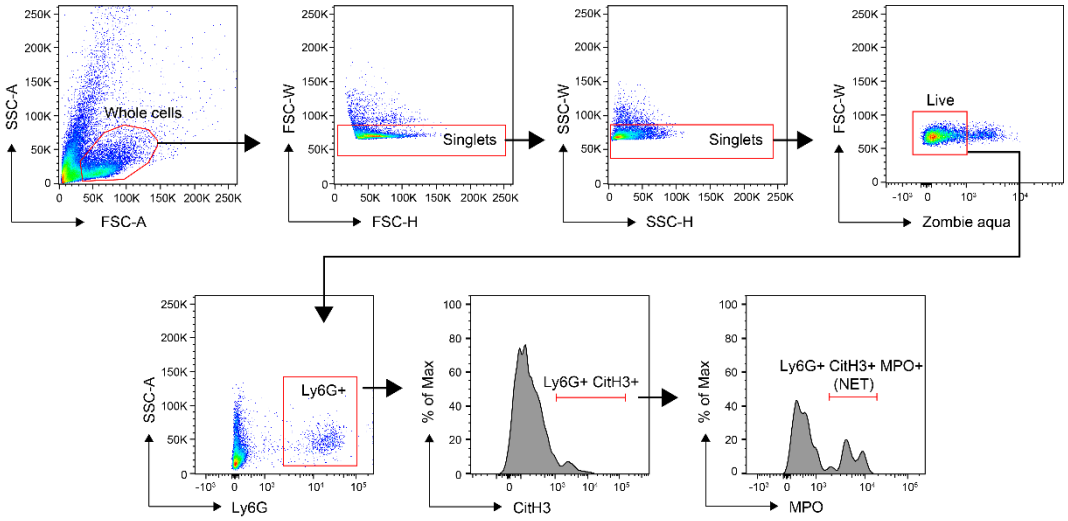

Figure 16. Gating scheme for identifying the Ly6G^{+}MPO^{+}CitH3^{+} NET population. Singlets were gated to avoid the unexpected false positive signal for fluorescence labeled antibody. The population of negative signal for Zombie Aqua dye was gated to identify live cell population. Within Ly6G^{+} neutrophils, CitH3^{+}MPO^{+} cell population was denoted formed NETs.

3.11. NLRP3 deficiency alleviates EAE severity at the disease peak

Next, this study confirmed the link between NLRP3 inflammasome and EAE progression, as previously reported[33]. This was evidenced by a reduction in clinical scores, prevention of weight loss, and decreased demyelination in the CNS of *Nlrp3* KO mice (Figure 17A–D). Although lack of NLRP3 alleviated the EAE severity, the number of infiltrated neutrophils in the CNS was indistinguishable between WT and *Nlrp3* KO mice at the EAE peak (Figure 17E and F). These findings have prompted us to consider the possibility that inflammasome may influence functionality of neutrophils, specifically NET formation, thereby potentially worsening the severity of EAE.

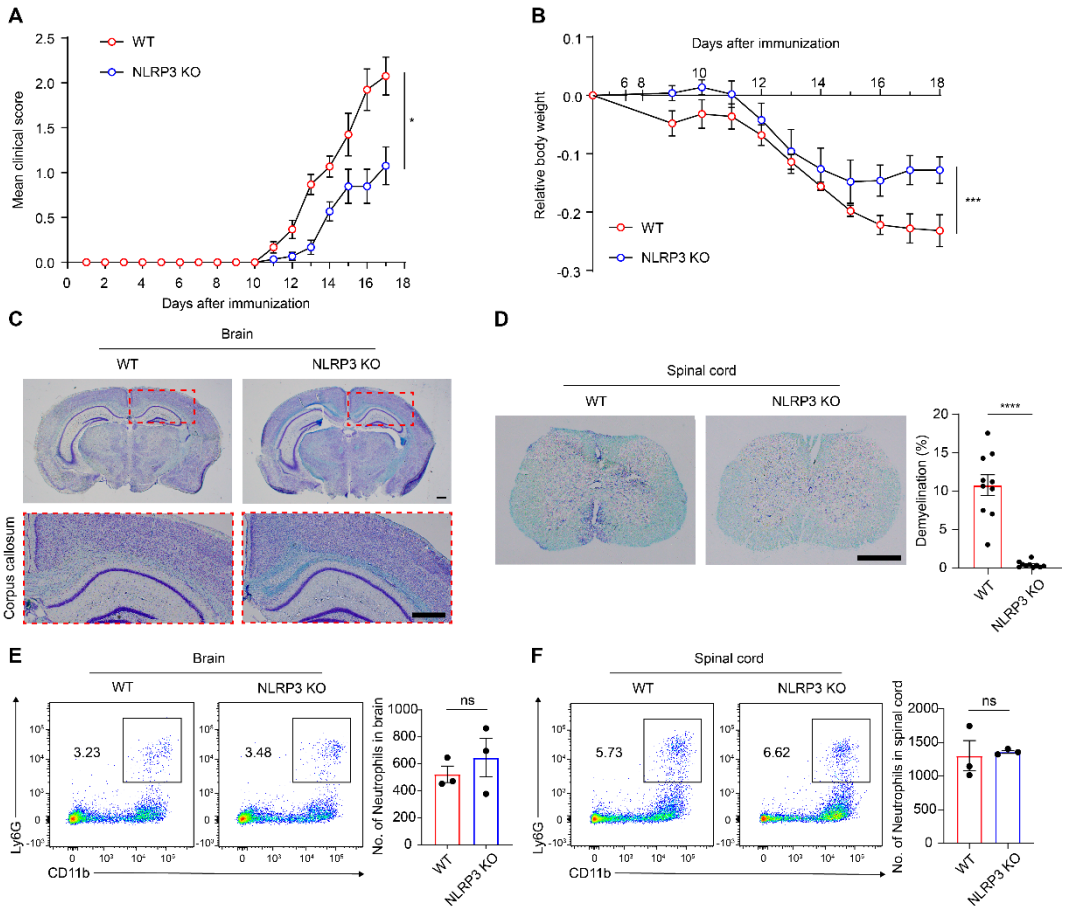

Figure 17. NLRP3 inflammasome contributes to the severity of EAE, although it is not essential for neutrophil infiltration at the peak of EAE. (A) Mean clinical score and (B) relative body weight of WT and *Nlrp3* KO groups. Demyelination of (C) brain or (D) spinal cord was analyzed using Luxol Fast Blue staining. (C) Top: coronal section images of brains. Bottom: enlarged corpus callosum. (D) Left: horizontal section images of spinal cord. Right: quantification of the percent value of demyelination. Scale bar: 500 μm. Scatter plots of leukocytes in (E) brains or (F) spinal cord and the number of neutrophils were presented. Data were shown with mean ± SEM. ns: non-significnat.

3.12. NLRP3 inflammasome promotes NET formation at the brain of EAE-induced mice

In our next investigation, we aimed to determine whether NLRP3 affects NET formation within the CNS during EAE progression. To identify differences in NET formation between WT and Nlrp3 KO mice at the peak of EAE, extracellular MPO and CitH3 levels in CNS-infiltrating neutrophils were assessed according to established protocols[23,80]. In the brain of *Nlrp3* KO, the expression levels of MPO and CitH3 on neutrophils were markedly decreased compared to WT (Figure 18A). Moreover, formed NETs ($Ly6G^+CitH3^+MPO^+$) were significantly diminished (Figure 18B). In the spinal cord, however, there was no difference in either the individual expression of MPO or CitH3, or in the released NET population between both mice (Figure 18C and D). These results imply that NLRP3 fosters the generation of NETs within the brain during EAE progression.

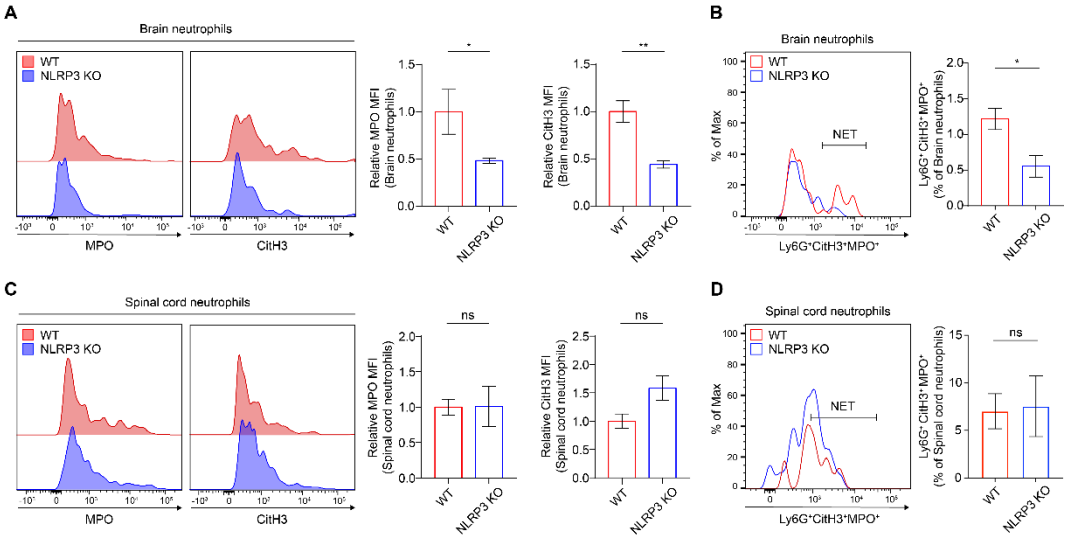

Figure 18. NLRP3 inflammasome promotes the generation of NETs during the progression of EAE predominantly in the brain. Relative MFI of individual expression level of NET components and the percentage of formed NETs on CNS-infiltrated neutrophils. (A) Histograms and relative MFI value of MPO and CitH3 of brain neutrophils in both groups. (B) Histograms and percentage of formed NETs of brain neutrophils. (C) Histograms and relative MFI value of MPO and CitH3 of spinal cord neutrophils in both groups. (D) Histograms and percentage of formed NETs of spinal cord neutrophils. Mean values are shown with error bars representing the SEM. MFI: mean fluorescence intensity. ns: non-significant.

3.13. NLRP3 inflammasome accumulates NETs in the brain in EAE pathogenesis

We further corroborated whether NLRP3-dependent NET formation accumulates in the brain. The results of this study identified that the lack of NLRP3 diminished accumulation of NET components in the brain of EAE-induced mice (Figure 19A). Supporting these observations, histological examination revealed fewer areas with NET component staining in *Nlrp3* KO mice (Figure 19B)[11,23]. Collectively, these results suggest a detrimental role of NLRP3 in the EAE by facilitating NET formation in the brain.

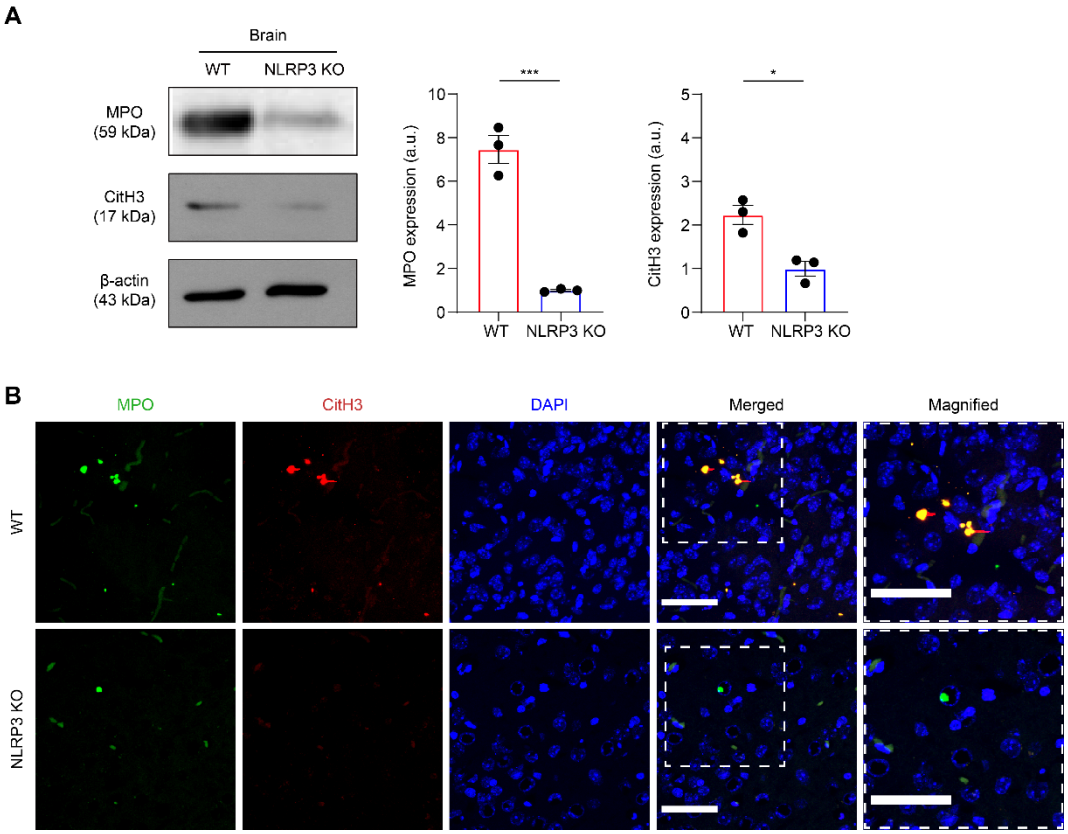

Figure 19. Emitted NETs accumulated in the brain. (A) Immunoblotting and quantification of NET components, including MPO and CitH3 in brains were presented. Protein levels were normalized against β-actin for accurate comparison. (B) Representative fluorescence microscopy images showing formed NETs in brains of both groups at EAE peak. Scale bar, 50 μm. Green: MPO. Red: CitH3. Blue: nuclei. Data were shown with mean ± SEM.

3.14. NLRP3 inflammasome contributes NET formation by increasing the expression of CXCR2, CXCR4, and CD63 on neutrophils during EAE pathogenesis

Given the decreased capacity for NET formation in the brain of *Nlrp3* KO, this study aimed to illuminate whether NLRP3 alters the phenotype of neutrophils associated with NET formation during pathogenesis of EAE. CXCR2 and CXCR4 have demonstrated NETs-associated surface molecules, as evidenced by findings that NETs were diminished through blocking either CXCR2[81] or CXCR4[82]. This study explored whether NLRP3 modifies these surface receptors on neutrophils during the EAE pathogenesis. In *Nlrp3* KO mice, brain neutrophils showed reduced expression of both CXCR2 and CXCR4 (Figure 20A). Additionally, circulating neutrophils exhibited diminished expression levels of both CXCR2 and CXCR4 (Figure 20B).

Degranulation, a hallmark of highly activated neutrophils, is crucial for releasing primary granules that contain components of NETs[8,83,84]. During degranulation, the membrane protein CD63, which is linked to intracellular granules, becomes more prominent on the surface of cells due to the merging of the plasma membrane with granules[83,85]. The capacity for degranulation in *Nlrp3* KO neutrophils was reduced in the brain and blood stream (Figure 20C and D). The findings support the hypothesis that NLRP3 modulates the phenotype of neutrophils, making them more predisposed to forming NETs during the progression of EAE.

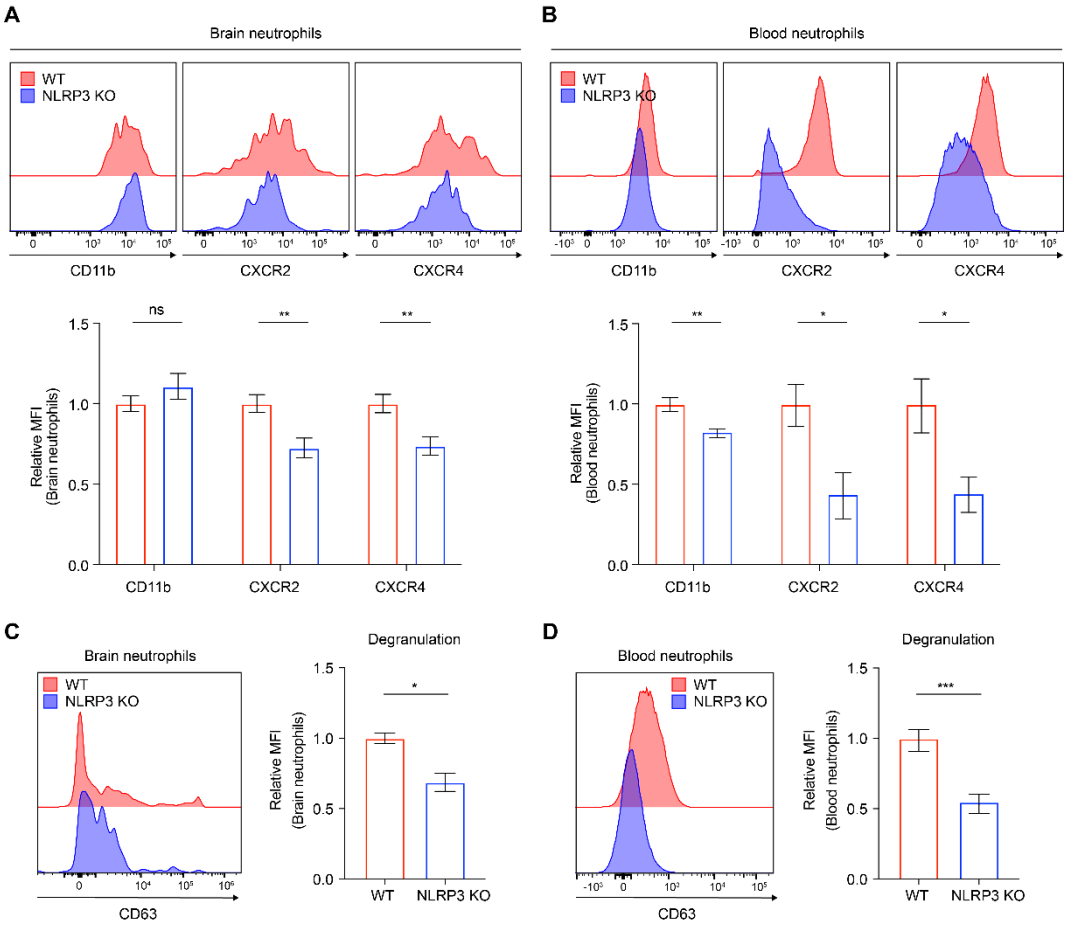

Figure 20. NLRP3 inflammasome enhances the expression of surface markers associated with NET formation, including CXCR2, CXCR4, and CD63. Histograms and relative MFI of CD11b, CXCR2, and CXCR4 of (A) brains or (B) blood neutrophils at peak disease. Histograms and relative MFI of CD63 of (C) brain or (D) blood neutrophils in both groups. MFI: mean fluorescence intensity. Data were reported as mean ± SEM. ns: non-significant.

3.15. NLRP3 inflammasome enhances the formation of NETs in the brains of EAE-induced mice via a mechanism that depends on ROS but is independent of PAD4

Next, this study aimed to clarify the molecular mechanisms underlying NET formation during EAE progression. Initially, the level of ROS was measured, as it is known to be linked to primed neutrophils and NET formation[83,86]. The influence of NLRP3 on ROS signaling during EAE progression was examined. Using DCFDA, a green fluorescent probe for ROS, the levels of ROS was measured in brain neutrophils[83,87]. Neutrophils in the brain of *Nlrp3* KO mice exhibited reduced ROS production at the peak of EAE (Figure 21A). We further determine *Hmox1* levels, a gene activated by ROS, in whole brain tissue[83,88]. Consistent with the reduced count of ROS^+ neutrophils, *Hmox1* expression was lower in *Nlrp3* KO mice (Figure 21B). These findings indicate that NLRP3 sustains ROS production, contributing to NET formation. While classical NET generation is dependent on ROS levels, there is also report of ROS-independent rapid NET formation[89]. Considering that PAD4 is a crucial enzyme for citrullinating histones during NET formation[90,91], the effect of NLRP3 on PAD4 levels in the brain was investigated. However, no notable differences in PAD4 levels were observed between these groups (Figure 21C-E). This discrepancy may result from the role of ROS in promoting the translocation of MPO[92,93], which further drives NET formation and leads to plasma membrane disruption. Consequently, these results indicate that NLRP3 promotes NET formation via a ROS-dependent mechanism and is independent of PAD4.

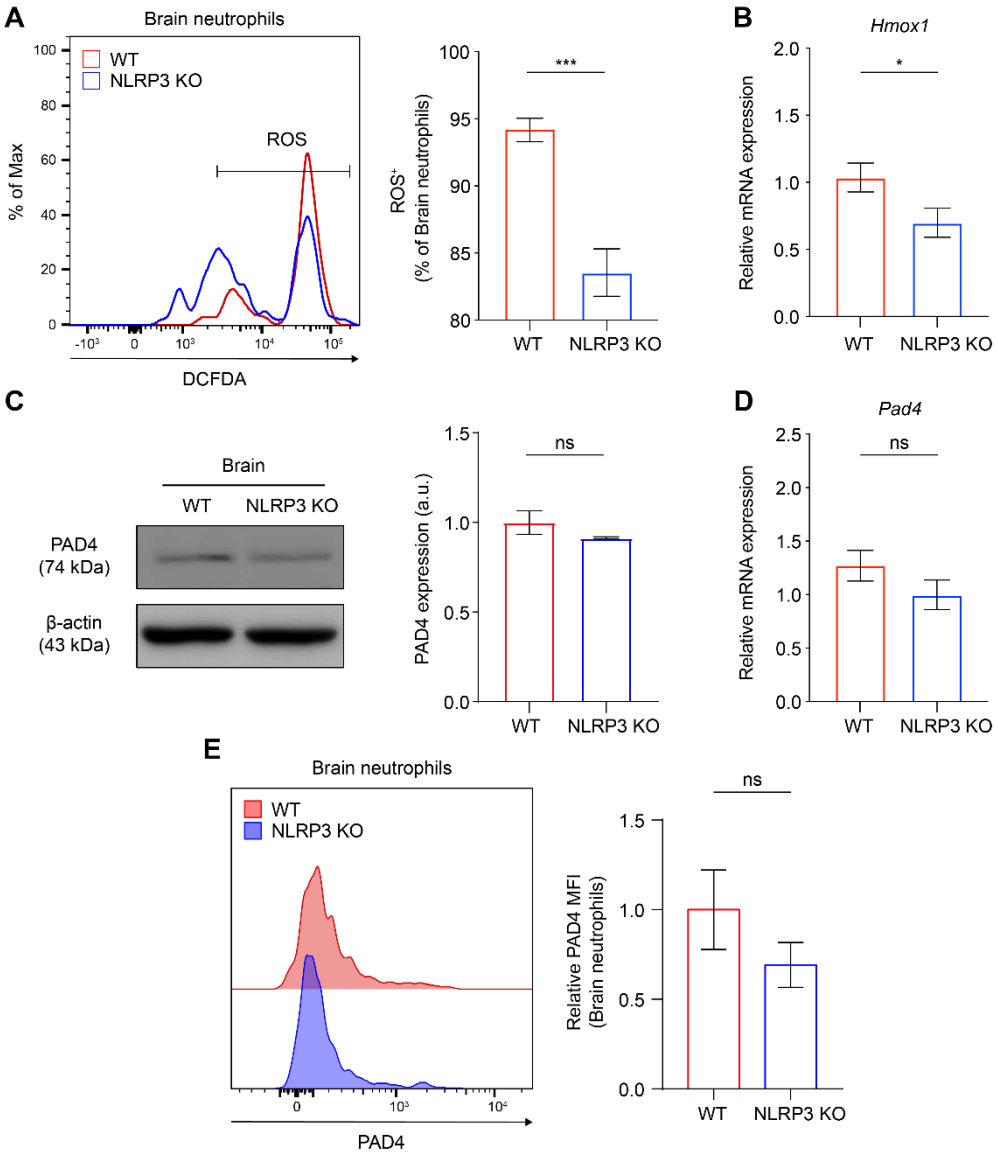

Figure 21. NLRP3 inflammasome facilitates the generation of NETs in a ROS-mediated manner, independently of PAD4. (A) Histogram and percentage value of ROS on brain neutrophils from both groups. (B and D) Relative mRNA expression level of *Hmox1* or *Pad4* in brains. (C) Immunoblotting and quantification of PAD4 in brains were

presented. (E) PAD4 expression on brain neutrophils represented by histogram analysis and relative MFI values. MFI: mean fluorescence intensity. Data were reported as mean ± SEM. ns: non-significant.

3.16. NETs exacerbate EAE severity by increasing the infiltration of T cells as EAE progression

Finally, to explore whether NLRP3-supported NET formation may exacerbate the severity of EAE, we used DNase1 to eliminate the accumulated NETs during the progression of EAE and investigated their potentially harmful effects. DNase1 was administered intraperitoneally 7 days after EAE induction, with injections occurring at 24 hr intervals[51,52]. The control group served as a reference point to determine the disease peak. In comparison to the control group, the DNase1 group exhibited a lower disease score and experienced less weight loss (Figure 22A and B). Consistent with the data on EAE severity, the removal of NETs alleviated demyelination (Figure 22C and D). These data suggest that NET elimination could attenuate the EAE severity. In addition to assessing symptom severity and the degree of demyelination, the impact of NETs on the recruitment of Th1 and Th17 cells, which significantly contribute to demyelination in this disease[94], was further examined. A reduction in the populations of $CD4^+IL\text{-}17A^+$, $CD4^+IFN\text{-}\gamma^+$, and $CD4^+IFN\text{-}\gamma^+IL\text{-}17A^+$ cells was identified in the CNS following DNase1 administration in EAE-induced mice (Figure 23A and B). In conclusion, these results suggest that NLRP3-mediated NET formation exacerbates EAE severity by enhancing the recruitment of Th1 and Th17 leukocytes to the CNS.

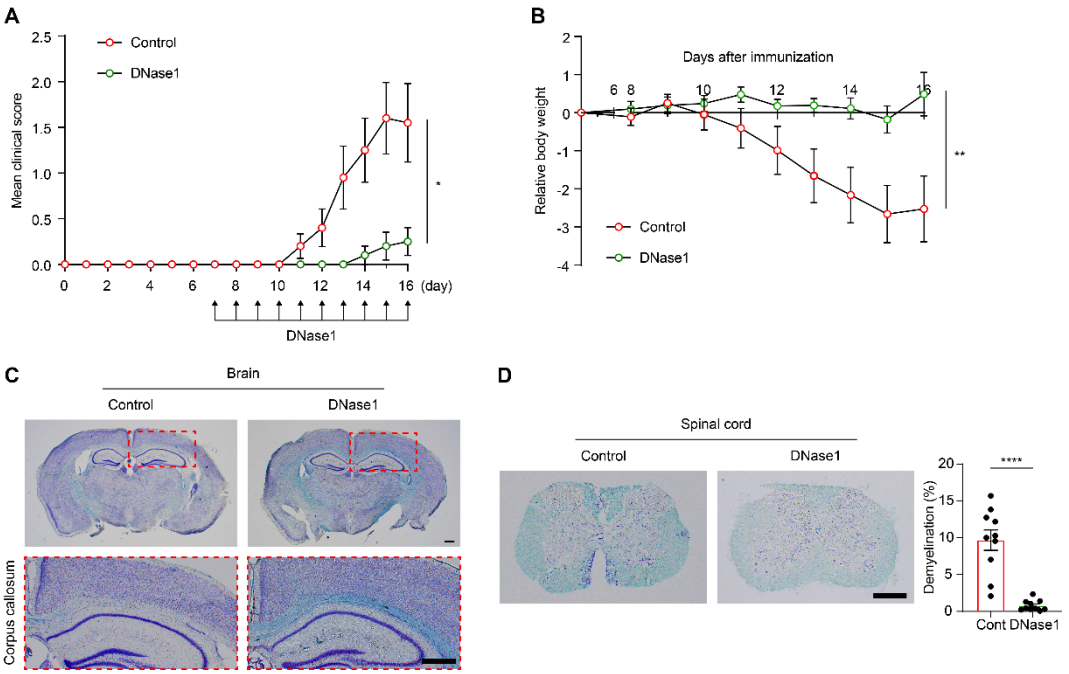

Figure 22. The elimination of NETs decreases the EAE severity. (A) EAE clinical score and (B) relative body weight of control and DNase1 groups. Demyelination of (C) brain or (D) spinal cord was evaluated using Luxol Fast Blue staining. (C) Top: coronal section images of brains. Bottom: enlarged corpus callosum. (D) Left: horizontal section images of spinal cord. Right: quantification of the percent value of demyelination. Data were shown with mean ± SEM. Scale bar, 500 μm.

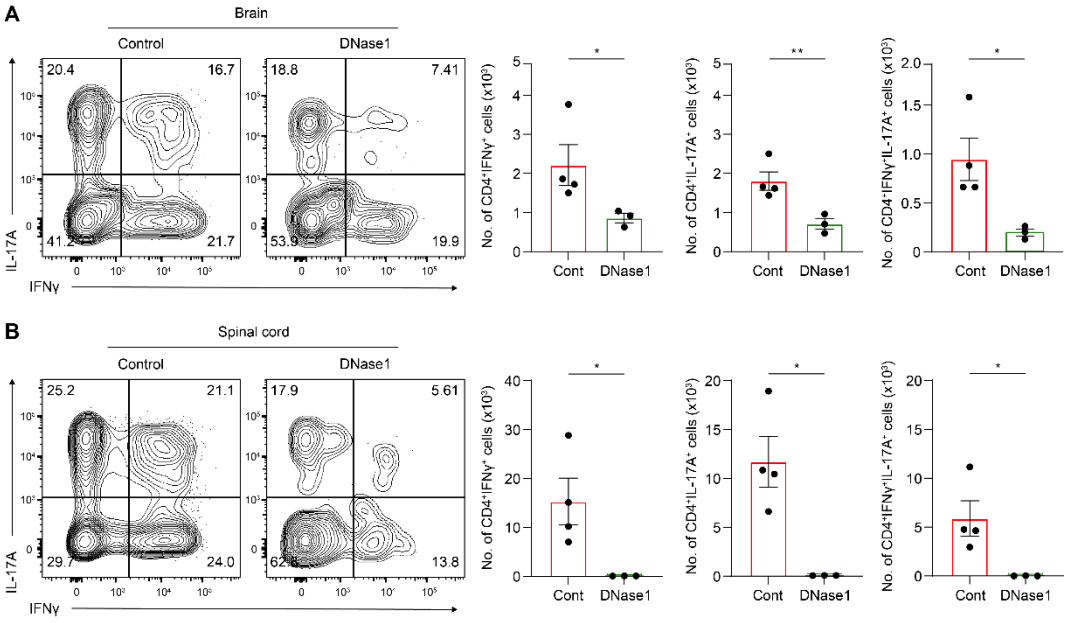

Figure 23. Eliminating NETs diminishes the infiltration of helper T lymphocytes into the CNS. Scatter plots of $CD4^+$ T cells and the absolute number of $CD4^+IL\text{-}17A^+$, $CD4^+IFN\gamma^+$, and $CD4^+IFN\gamma^+IL\text{-}17A^+$ cells in (A) brains or (B) spinal cord. Data were shown with mean ± SEM.

4. DISCUSSION

The two important findings of PART I in this study were that 1) neutrophils mainly contribute to initial neuroinflammation through NLRP3 expression, and 2) NLRP3 activation in neutrophils leads to the activation of the CXCL1/2-CXCR2 axis signaling, which facilitates neutrophil infiltration and BBB disruption, revealing that this axis is crucial for EAE progression. The results of this study add new components to the cascade of molecular mechanisms that contribute to neutrophil infiltration in the inflamed brain.

NLRP3 inflammasome promotes neutrophil infiltration to brain in this study. Our findings agree with the findings of previous studies, which reported that NLRP3 inflammasome contributes to neutrophil infiltration in the inflamed brain[28,95]. Moreover, NLRP3 inflammasome induces BBB disintegration, corresponding to previous studies that reported NLRP3 inhibition preserves BBB integrity in several pathological mice model[96-98]. In accordance with our results, recent study has shown that the neutrophil infiltration and the BBB disruption are observed concurrently in inflammatory conditions[19]. It has also demonstrated that the number of infiltrated neutrophils directly correlates with vascular leakage[19]. While these findings suggest that neutrophil transmigration is associated with BBB permeability, it is unclear whether increased BBB permeability directly promotes neutrophil infiltration. Taken together, the current findings indicate that the NLRP3 inflammasome enhances neuroinflammation including neutrophil infiltration to brain and BBB disintegration. A future study of the relationship between the changes in BBB

permeability by NLRP3 inflammasome and the neutrophil infiltration needs to be conducted.

The findings of this study show that brain neutrophils exhibited an elevation in the levels of NLRP3 and CD11b at the early stages of neuroinflammation, but other immune cells including $Ly6C^{hi}$, $Ly6C^{low}$, and microglia showed no changes (Figure 6A, 6B, 7A, and 7B). This suggests that neutrophils could mainly contribute to initial neuroinflammation through NLRP3 expression. A previous study reported that prophylactic anti-Ly6G treatment effectively diminished neutrophil infiltration and significantly reduced pro-inflammatory cytokine levels. In contrast, administering anti-Ly6G treatment 4 hours after hypoxic-ischemic encephalopathy (HIE) was ineffective in preventing neutrophil infiltration and brain damage, highlighting the pathological role of early-arriving neutrophils in inflammation-sensitized HIE[99]. These results supported our hypothesis that neutrophils play essential role in the initial neuroinflammation. Our results also displayed that NLRP3-deficient neutrophils showed a primed phenotype at early stages of LPS-induced neuroinflammation, but eventually failed to infiltrate to inflamed brain (Figure 1D, 1E, and 6B). These results indicate that NLRP3 is dispensable for neutrophil priming, but required for the neutrophil infiltration to inflamed brain.

NLRP3 activation in neutrophils can trigger neutrophil infiltration to brain in this study. This result aligns with the findings previously reported by Stackowicz *et al*.[63], who reported that NLRP3 activation in neutrophils triggers skin inflammation including recruitment of neutrophil in the skin. Additionally, Kaufmann *et al*.[36] have shown that

activation of NLRP3 in neutrophils triggers inflammation in the liver, including accumulation of inflammatory cytokine and infiltrating neutrophils. Overall, these findings demonstrate that NLRP3 activation in neutrophils could initiate the neutrophil infiltration to several organs. Our results also showed that NLRP3 activation in neutrophils triggers BBB disintegration, thereby increasing its permeability. Numerous studies have demonstrated that activated neutrophils increase vascular permeability[58,100-102]. Furthermore, previous studies reported that neutrophil depletion alleviates BBB breakdown in inflamed brain[51,103]. This finding aligns with the hypothesis that activated neutrophils contribute BBB disintegration, increasing vascular permeability. Taken together, NLRP3 activation in neutrophils can trigger neuroinflammation including the neutrophil infiltration to brain and the BBB disruption.

The chemokines CXCL1 and CXCL2 serve as mediators between NLRP3 activation in neutrophils and BBB disintegration in this study. The function of chemokines now extends well beyond their initial characterization as leukocyte chemoattractants[65,104,105]. Haarmann *et al*.[106] demonstrated that both CXCL5 and CXCL8 impair the integrity of the paracellular barrier in human brain endothelial monolayer. Yu *et al*.[107] found that the permeability of human endothelium was increased by CXCL8 through the downregulation of tight junctions. These findings support our hypothesis that chemokines would contribute to BBB dysfunction via reducing BBB integrity. In this study, NLRP3 activated neutrophils increased both CXCL1 and CXCL2 production (Figure 10A). Both chemokines reduced BBB integrity (Figure 10C). The results are coherent with the findings of previous study,

which reported that neutrophils emerged as the primary producers of CXCL2, and this chemokine plays critical role for correct breaching of endothelial junctions[65]. Interestingly, our findings showed that both CXCL1 and CXCL2 reduced the expression of extracellular Claudin-5, whereas no change was observed in the expression of intracellular ZO-1 on brain endothelium *in vitro* (Figure 10C). The differences may be attributed to the cellular localization of these junctional proteins in endothelial cells. Considering all of these, our findings provide evidence that both CXCL1 and CXCL2 contribute to BBB dysfunction by reducing extracellular Claudin-5 on brain endothelium.

Astrocytes, pericytes, neutrophils, and endothelial cells express CXCL1 and CXCL2, as observed *in vivo* by their co-localization with $GFAP^+$ astrocytes, $NG2^+$ pericytes, $LysM^+$ neutrophils, and $CD31^+$ endothelial cells following LPS injection. This observation is consistent with previous studies, which have also reported that activated astrocytes[108,109], pericytes[110], neutrophils[111,112], and endothelial cells[113] express the chemokines CXCL1 and CXCL2 in response to LPS. Thus, in the neuroinflammation triggered by systemic inflammation, these chemokine signaling pathways are activated by various cells, contributing to BBB dysfunction.

CXCR2, a cognate receptor for CXCL1 and CXCL2, is critical for regulating neutrophil infiltration and BBB permeability in this study. The blockade of CXCR2 reduced neutrophil infiltration and the vascular permeability in brains (Figure 13A-D). This finding agrees with the findings of previous studies, which reported that following LPS injection, neutrophil infiltration was reduced by blocking CXCR2[109,114,115], CXCL1[109], or

CXCL2[116]. Furthermore, it has been reported that following herpes simplex virus (HSV) infection, BBB permeability was reduced by blocking CXCR2 or CXCL1[19]. As mentioned above, CXCL1, CXCL2, CXCL5, and CXCL8 contribute to BBB dysfunction by reducing BBB integrity[106,107]. Considering that these chemokines are ligands of CXCR2, CXCR2 signaling is crucial for regulating BBB integrity.

Given that CXCR2 is pivotal for neutrophil intravasation from BM to bloodstream[117], it can also be considered that blockade of CXCR2 inhibits neutrophil intravasation, thereby contributing to a decrease in neutrophil extravasation to inflamed brain. A recent study has demonstrated that the antagonist injected intraperitoneally modulates bone marrow stromal cells[118]. It is inferred that the antagonist is delivered to the BM through the bloodstream. Since molecules with a molecular weight of less than 400 Da can cross the BBB[119], the CXCR2 antagonist, with a molecular weight of 352 Da, can penetrate blood vessels, including BBB. Therefore, the antagonist may lower the count of migrating neutrophils from BM to the bloodstream, potentially reducing brain-infiltrating neutrophils by interrupting the sequential migration process through the bone marrow, bloodstream, and inflamed brain.

EAE, a mouse model for studying multiple sclerosis, is autoimmune demyelinating disease affecting CNS[29,30]. Neutrophil infiltration into the CNS at the onset of EAE has been shown to contribute to disease progression. This is supported by findings that neutrophil depletion prior to disease onset significantly reduces EAE severity, whereas depletion after onset failed to alleviate disease

severity[14]. The results of this study indicate that the active mutant increased both the clinical score and the incidence of EAE while accelerating disease onset in a CXCR2-dependent manner. Moreover, the active mutant enhanced neutrophil infiltration to the brain through CXCR2 signaling. To sum up, our findings suggest that NLRP3 activation in neutrophils exacerbates EAE progression via CXCR2-mediated neutrophil infiltration.

There are some limitations to PART I in this study. We identified that CXCR2 signaling promotes neutrophil infiltration and BBB disruption in neuroinflammation models induced by LPS or by NLRP3 activation in neutrophils. Therefore, further investigation is required to generalize the current results to neuroinflammation models induced by other factors. However, some studies have reported the effect of CXCR2 signaling on neutrophil infiltration and BBB disruption following HSV or *S. pneumoniae* infection[19,120]. Thus, this study can provide additional evidence supporting the essential function of CXCR2 signaling in regulating the infiltration and BBB disruption.

The two important findings of PART II in this study were that 1) during EAE pathogenesis, neutrophils infiltrate the CNS and form NETs, leading to their accumulation, and 2) NLRP3 inflammasome promotes NET generation in brains, exacerbating EAE severity by facilitating the infiltration of T lymphocytes to the CNS and contributing demyelination.

A recent study has demonstrated that emitted DNA triggers activation of the inflammasome, as evidenced by inflammasome activation mediated by DNA released from

neutrophils[121]. The results of this study indicate that NLRP3 promotes NET formation. Considering these findings, there is a detrimental feedback loop between NET formation and NLRP3 in neutrophils[23,122,123]. NLRP3 is activated during EAE progression, resulting in an increase in NETs. The formed NETs, in turn, may trigger NLRP3 activation. Hence, it is proposed that NET-associated surface molecules, including CXCR2, CXCR4, and CD63, which are upregulated by NLRP3, can amplify the vicious cycle. In addition, the NLRP3 inflammasome affects the expression of CD11b in specifically circulating neutrophils. This finding could imply that CD11b on neutrophils plays a differential role based on their location and phase of migration, as highlighted by previous studies[124-127].

The results in this study showed that NET elimination using DNase1 effectively alleviated the EAE score, weight loss, and demyelination. Additionally, DNase1 reduced the numbers of $CD4^+IL\text{-}17A^+$, $CD4^+IFN\text{-}\gamma^+$, and $CD4^+IFN\text{-}\gamma^+IL\text{-}17A^+$ cells in the CNS. Previous studies have suggested that Th17 lymphocytes have the capacity for producing both IL-17A and IFN-γ during EAE. These IFN-γ producing Th17 cells exhibit characteristics that are more akin to Th1 rather than Th17 cells in transfer EAE[128,129]. The data in this study imply that generated NETs modulate the inflammatory environment by interacting with T cells in the brain. However, the exact mechanisms by which this occurs require further investigation. The current findings suggest three potential mechanisms explaining the relationship between T cells and NETs in the progression of EAE. First, NETs lower the threshold for CD4 T cell activation, leading to their priming[130]. Second, NETs and the related histone complexes have been shown to promote Th17 cell

differentiation[130,131]. Finally, antigen-presenting cells (APCs) detect the released NETs and present to T cells as self-antigens. Subsequently, the activated T cells produce GM-CSF and IL-17, promoting further neutrophil infiltration and activation, ultimately establishing a vicious cycle[132,133].

Neutrophils contribute to the progression of EAE through cytokine production, BBB disruption, and releasing NETs[134]. During EAE, neutrophils produce proinflammatory cytokines that promote the maturation of APCs, thereby facilitating reactivation of T cells within the interstitium. This is evidenced by findings that neutrophils isolated from the CNS at disease onset increased the APC phenotypes of bone marrow-derived dendritic cells during co-culture[14]. Furthermore, depletion of neutrophils before onset decreased the APC phenotypes of monocytes/macrophages and microglia in the CNS[14]. While the precise mechanisms by which neutrophils disrupt the BBB are not fully understood, neutrophil depletion contributes to preserving BBB integrity[135,136]. Finally, brain infiltrated neutrophils induced releasing NETs, which contributes to neuronal cell death[137]. The results of this study also indicate that during EAE, emitted NETs increased the infiltration of Th1 and Th17 lymphocytes, leading to demyelination in the CNS. In turn, neutrophils could be a potential target for therapeutic approaches to attenuate EAE severity by modulating T cell reactivation, BBB disruption, and demyelination.

NLRP3 inflammasome matures also IL-18 through the activation of caspase-1[22]. A previous study has reported that peripheral mononuclear cells from MS patients, including those with secondary progressive or relapsing-remitting MS, have an enhanced

capacity for producing IL-18 via the CD40-CD40L interaction between $CD4^+$ T lymphocytes and APCs[138]. The blockade of IL-18 using KO mice or neutralizing antibodies ameliorated the severity of demyelinating disease[139,140]. In contrast, the intraperitoneal injection of IL-18 increased the EAE clinical score in WT mice, and induced a resurgence of symptoms in IL-18 KO mice[139]. On this basis, NLRP3 prevention may contribute to alleviating the EAE severity by reducing IL-18 production, as well as by suppressing NET formation.

The results of this study need to be interpreted with certain limitations. Specifically, the NLRP3 inflammasome enhanced ROS-mediated NET formation in brain but showed no effect within spinal cord. It is unknown why NLRP3 had such an insignificant effect on the spinal cord. However, given that previous research reported the subtle progression of EAE in various anatomic regions, it is plausible that distinct microenvironmental factors within these anatomical regions play a role in influencing NET formation driven by NLRP3[141]. Additionally, it is crucial to note that the method used in this study to eliminate NETs has limitations for assessing NET function, particularly in the brain, as it removes NETs systemically throughout the entire body, not just in the brain. This could explain why DNase1 is more effective at reducing EAE symptoms than it is when NLRP3 is absent. Consequently, it is still unclear how increased NLRP3-formed NETs in the brain affect the progression of EAE, even though our research showed that NETs influence the disease progression and the recruitment of Th1 and Th17.

5. CONCLUSION

This study elucidates that NLRP3 activation in neutrophils triggers neuroinflammation, including neutrophil infiltration and BBB disruption, via the secretion of CXCL1/2 and subsequent activation of the CXCL1/2-CXCR2 axis signaling. These CXCL1/2 chemokines are produced by astrocytes, pericytes, neutrophils, and endothelial cells in the LPS-elicited neuroinflammation. Furthermore, blockade of CXCR2 signaling attenuates neutrophil infiltration and BBB disruption in the neuroinflammation models induced by LPS or by NLRP3 activation in neutrophils. Thus, this chemokine axis could be a potential target for therapeutic approaches to attenuate neuroinflammation by modulating neutrophil infiltration and BBB disruption. Moreover, this study identifies infiltrated neutrophils and formed NETs in the CNS at the EAE peak. In particular, this study indicates that NETs are an etiological factor in EAE, aggravating demyelination and EAE severity by increasing the recruitment of Th1 and Th17 cells.

Altogether, this study provides evidence that NLRP3 modulates the migration patterns and functional phenotypes of neutrophils, enhancing their infiltration and ROS-mediated NET formation in brain tissue. In addition, NLRP3 activation in neutrophils induces CXCR2-mediated BBB disruption. Thus, NLRP3 intervention could be considered a therapeutic approach to mitigate BBB disruption, neutrophil infiltration, and NET generation in brain, thereby alleviating EAE pathogenesis.

REFERENCES

1. Chevre R, Soehnlein O. Neutrophil life in three acts: a production by different stage directors. Nat Immunol 2021;22:1072-4.
2. Rosales C. Neutrophil: A Cell with Many Roles in Inflammation or Several Cell Types? Front Physiol 2018;9:113.
3. Liew PX, Kubes P. The Neutrophil's Role During Health and Disease. Physiol Rev 2019;99:1223-48.
4. Tecchio C, Cassatella MA. Neutrophil-derived chemokines on the road to immunity. Semin Immunol 2016;28:119-28.
5. Greenlee-Wacker MC. Clearance of apoptotic neutrophils and resolution of inflammation. Immunol Rev 2016;273:357-70.
6. von Leden RE, Parker KN, Bates AA, Noble-Haeusslein LJ, Donovan MH. The emerging role of neutrophils as modifiers of recovery after traumatic injury to the developing brain. Exp Neurol 2019;317:144-54.
7. Rumble JM, Huber AK, Krishnamoorthy G, Srinivasan A, Giles DA, Zhang X, et al. Neutrophil-related factors as biomarkers in EAE and MS. J Exp Med 2015;212:23-35.
8. Naegele M, Tillack K, Reinhardt S, Schippling S, Martin R, Sospedra M. Neutrophils in multiple sclerosis are characterized by a primed phenotype. J Neuroimmunol 2012;242:60-71.
9. Perez-de-Puig I, Miró-Mur F, Ferrer-Ferrer M, Gelpi E, Pedragosa J, Justicia C,

et al. Neutrophil recruitment to the brain in mouse and human ischemic stroke. Acta Neuropathol 2015;129:239-57.

10. Weisenburger-Lile D, Dong Y, Yger M, Weisenburger G, Polara GF, Chaigneau T, et al. Harmful neutrophil subsets in patients with ischemic stroke: Association with disease severity. Neurol Neuroimmunol Neuroinflamm 2019;6:e571.
11. Zenaro E, Pietronigro E, Della Bianca V, Piacentino G, Marongiu L, Budui S, et al. Neutrophils promote Alzheimer's disease-like pathology and cognitive decline via LFA-1 integrin. Nat Med 2015;21:880-6.
12. Rossi B, Santos-Lima B, Terrabuio E, Zenaro E, Constantin G. Common Peripheral Immunity Mechanisms in Multiple Sclerosis and Alzheimer's Disease. Front Immunol 2021;12:639369.
13. Wang C, Börger V, Sardari M, Murke F, Skuljec J, Pul R, et al. Mesenchymal Stromal Cell-Derived Small Extracellular Vesicles Induce Ischemic Neuroprotection by Modulating Leukocytes and Specifically Neutrophils. Stroke 2020;51:1825-34.
14. Steinbach K, Piedavent M, Bauer S, Neumann JT, Friese MA. Neutrophils amplify autoimmune central nervous system infiltrates by maturing local APCs. J Immunol 2013;191:4531-9.
15. Vestweber D. Adhesion and signaling molecules controlling the transmigration of leukocytes through endothelium. Immunol Rev 2007;218:178-96.
16. Carman CV, Sage PT, Sciuto TE, de la Fuente MA, Geha RS, Ochs HD, et al.

Transcellular diapedesis is initiated by invasive podosomes. Immunity 2007;26:784-97.

17. Veldhuis WB, Floris S, van der Meide PH, Vos IM, de Vries HE, Dijkstra CD, et al. Interferon-beta prevents cytokine-induced neutrophil infiltration and attenuates blood-brain barrier disruption. J Cereb Blood Flow Metab 2003;23:1060-9.

18. McKittrick CM, Lawrence CE, Carswell HV. Mast cells promote blood brain barrier breakdown and neutrophil infiltration in a mouse model of focal cerebral ischemia. J Cereb Blood Flow Metab 2015;35:638-47.

19. Michael BD, Bricio-Moreno L, Sorensen EW, Miyabe Y, Lian J, Solomon T, et al. Astrocyte- and Neuron-Derived CXCL1 Drives Neutrophil Transmigration and Blood-Brain Barrier Permeability in Viral Encephalitis. Cell Rep 2020;32:108150.

20. McColl SR, St-Onge M, Dussault AA, Laflamme C, Bouchard L, Boulanger J, et al. Immunomodulatory impact of the A2A adenosine receptor on the profile of chemokines produced by neutrophils. Faseb j 2006;20:187-9.

21. Scapini P, Lapinet-Vera JA, Gasperini S, Calzetti F, Bazzoni F, Cassatella MA. The neutrophil as a cellular source of chemokines. Immunol Rev 2000;177:195-203.

22. Swanson KV, Deng M, Ting JP. The NLRP3 inflammasome: molecular activation and regulation to therapeutics. Nat Rev Immunol 2019;19:477-89.

23. Byun DJ, Lee J, Yu JW, Hyun YM. NLRP3 Exacerbate NETosis-Associated Neuroinflammation in an LPS-Induced Inflamed Brain. Immune Netw 2023;23:e27.

24. Byun DJ, Lee J, Ko K, Hyun YM. NLRP3 exacerbates EAE severity through ROS-dependent NET formation in the mouse brain. Cell Commun Signal 2024;22:96.

25. Inoue Y, Shirasuna K, Kimura H, Usui F, Kawashima A, Karasawa T, et al. NLRP3 regulates neutrophil functions and contributes to hepatic ischemia-reperfusion injury independently of inflammasomes. J Immunol 2014;192:4342-51.

26. Amaral FA, Costa VV, Tavares LD, Sachs D, Coelho FM, Fagundes CT, et al. NLRP3 inflammasome-mediated neutrophil recruitment and hypernociception depend on leukotriene B(4) in a murine model of gout. Arthritis Rheum 2012;64:474-84.

27. Fukui S, Fukui S, Van Bruggen S, Shi L, Sheehy CE, Chu L, et al. NLRP3 inflammasome activation in neutrophils directs early inflammatory response in murine peritonitis. Sci Rep 2022;12:21313.

28. Miraglia MC, Costa Franco MM, Rodriguez AM, Bellozi PM, Ferrari CC, Farias MI, et al. Glial Cell-Elicited Activation of Brain Microvasculature in Response to Brucella abortus Infection Requires ASC Inflammasome-Dependent IL-1β Production. J Immunol 2016;196:3794-805.

29. Sawcer S, Hellenthal G, Pirinen M, Spencer CC, Patsopoulos NA, Moutsianas L, et al. Genetic risk and a primary role for cell-mediated immune mechanisms in multiple sclerosis. Nature 2011;476:214-9.

30. Dendrou CA, Fugger L, Friese MA. Immunopathology of multiple sclerosis. Nat Rev Immunol 2015;15:545-58.

31. McGinley AM, Edwards SC, Raverdeau M, Mills KHG. Th17 cells, γδ T cells and their interplay in EAE and multiple sclerosis. J Autoimmun 2018; doi:10.1016/j.jaut.2018.01.001.

32. Zhang Z, Ma Q, Velagapudi R, Barclay WE, Rodriguiz RM, Wetsel WC, et al. Annexin-A1 Tripeptide Attenuates Surgery-Induced Neuroinflammation and Memory Deficits Through Regulation the NLRP3 Inflammasome. Front Immunol 2022;13:856254.

33. Inoue M, Williams KL, Gunn MD, Shinohara ML. NLRP3 inflammasome induces chemotactic immune cell migration to the CNS in experimental autoimmune encephalomyelitis. Proc Natl Acad Sci U S A 2012;109:10480-5.

34. Hou B, Zhang Y, Liang P, He Y, Peng B, Liu W, et al. Inhibition of the NLRP3-inflammasome prevents cognitive deficits in experimental autoimmune encephalomyelitis mice via the alteration of astrocyte phenotype. Cell Death Dis 2020;11:377.

35. Ma JH, Lee E, Yoon SH, Min H, Oh JH, Hwang I, et al. Therapeutic effect of NLRP3 inhibition on hearing loss induced by systemic inflammation in a CAPS-

associated mouse model. EBioMedicine 2022;82:104184.

36. Kaufmann B, Leszczynska A, Reca A, Booshehri LM, Onyuru J, Tan Z, et al. NLRP3 activation in neutrophils induces lethal autoinflammation, liver inflammation, and fibrosis. EMBO Rep 2022;23:e54446.

37. Diana J, Lehuen A. Macrophages and β-cells are responsible for CXCR2-mediated neutrophil infiltration of the pancreas during autoimmune diabetes. EMBO Mol Med 2014;6:1090-104.

38. Pino PA, Cardona AE. Isolation of brain and spinal cord mononuclear cells using percoll gradients. J Vis Exp 2011; doi:10.3791/2348.

39. Korin B, Dubovik T, Rolls A. Mass cytometry analysis of immune cells in the brain. Nat Protoc 2018;13:377-91.

40. Anderson KG, Mayer-Barber K, Sung H, Beura L, James BR, Taylor JJ, et al. Intravascular staining for discrimination of vascular and tissue leukocytes. Nat Protoc 2014;9:209-22.

41. Kim YR, Kim YM, Lee J, Park J, Lee JE, Hyun YM. Neutrophils Return to Bloodstream Through the Brain Blood Vessel After Crosstalk With Microglia During LPS-Induced Neuroinflammation. Front Cell Dev Biol 2020;8:613733.

42. Park J, Kim JY, Kim YR, Huang M, Chang JY, Sim AY, et al. Reparative System Arising from CCR2(+) Monocyte Conversion Attenuates Neuroinflammation Following Ischemic Stroke. Transl Stroke Res 2021;12:879-93.

43. Lee S, Kang BM, Kim JH, Min J, Kim HS, Ryu H, et al. Real-time in vivo two-

photon imaging study reveals decreased cerebro-vascular volume and increased blood-brain barrier permeability in chronically stressed mice. Sci Rep 2018;8:13064.

44. Haruwaka K, Ikegami A, Tachibana Y, Ohno N, Konishi H, Hashimoto A, et al. Dual microglia effects on blood brain barrier permeability induced by systemic inflammation. Nat Commun 2019;10:5816.

45. Lim K, Sumagin R, Hyun YM. Extravasating Neutrophil-derived Microparticles Preserve Vascular Barrier Function in Inflamed Tissue. Immune Netw 2013;13:102-6.

46. Han YW, Choi JY, Uyangaa E, Kim SB, Kim JH, Kim BS, et al. Distinct dictation of Japanese encephalitis virus-induced neuroinflammation and lethality via triggering TLR3 and TLR4 signal pathways. PLoS Pathog 2014;10:e1004319.

47. Wang T, Town T, Alexopoulou L, Anderson JF, Fikrig E, Flavell RA. Toll-like receptor 3 mediates West Nile virus entry into the brain causing lethal encephalitis. Nat Med 2004;10:1366-73.

48. Braniste V, Al-Asmakh M, Kowal C, Anuar F, Abbaspour A, Tóth M, et al. The gut microbiota influences blood-brain barrier permeability in mice. Sci Transl Med 2014;6:263ra158.

49. El-Behi M, Ciric B, Dai H, Yan Y, Cullimore M, Safavi F, et al. The encephalitogenicity of T(H)17 cells is dependent on IL-1- and IL-23-induced production of the cytokine GM-CSF. Nat Immunol 2011;12:568-75.

50. Kim GR, Kim WJ, Lim S, Lee HG, Koo JH, Nam KH, et al. In Vivo Induction of Regulatory T Cells Via CTLA-4 Signaling Peptide to Control Autoimmune Encephalomyelitis and Prevent Disease Relapse. Adv Sci (Weinh) 2021;8:2004973.

51. Kang L, Yu H, Yang X, Zhu Y, Bai X, Wang R, et al. Neutrophil extracellular traps released by neutrophils impair revascularization and vascular remodeling after stroke. Nat Commun 2020;11:2488.

52. Wang R, Zhu Y, Liu Z, Chang L, Bai X, Kang L, et al. Neutrophil extracellular traps promote tPA-induced brain hemorrhage via cGAS in mice with stroke. Blood 2021;138:91-103.

53. Miyauchi E, Kim SW, Suda W, Kawasumi M, Onawa S, Taguchi-Atarashi N, et al. Gut microorganisms act together to exacerbate inflammation in spinal cords. Nature 2020;585:102-6.

54. Wendeln AC, Degenhardt K, Kaurani L, Gertig M, Ulas T, Jain G, et al. Innate immune memory in the brain shapes neurological disease hallmarks. Nature 2018;556:332-8.

55. Bittner-Eddy PD, Fischer LA, Tu AA, Allman DA, Costalonga M. Discriminating between Interstitial and Circulating Leukocytes in Tissues of the Murine Oral Mucosa Avoiding Nasal-Associated Lymphoid Tissue Contamination. Front Immunol 2017;8:1398.

56. Hidalgo A, Chilvers ER, Summers C, Koenderman L. The Neutrophil Life Cycle.

Trends Immunol 2019;40:584-97.

57. Zhang X, Tang X, Ma F, Fan Y, Sun P, Zhu T, et al. Endothelium-targeted overexpression of Krüppel-like factor 11 protects the blood-brain barrier function after ischemic brain injury. Brain Pathol 2020;30:746-65.

58. Santos-Lima B, Pietronigro EC, Terrabuio E, Zenaro E, Constantin G. The role of neutrophils in the dysfunction of central nervous system barriers. Front Aging Neurosci 2022;14:965169.

59. Spiteri AG, Terry RL, Wishart CL, Ashhurst TM, Campbell IL, Hofer MJ, et al. High-parameter cytometry unmasks microglial cell spatio-temporal response kinetics in severe neuroinflammatory disease. J Neuroinflammation 2021;18:166.

60. Puga I, Cols M, Barra CM, He B, Cassis L, Gentile M, et al. B cell-helper neutrophils stimulate the diversification and production of immunoglobulin in the marginal zone of the spleen. Nat Immunol 2011;13:170-80.

61. Boschmann M, Engeli S, Adams F, Gorzelniak K, Franke G, Klaua S, et al. Adipose tissue metabolism and CD11b expression on monocytes in obese hypertensives. Hypertension 2005;46:130-6.

62. Böttcher C, Schlickeiser S, Sneeboer MAM, Kunkel D, Knop A, Paza E, et al. Human microglia regional heterogeneity and phenotypes determined by multiplexed single-cell mass cytometry. Nat Neurosci 2019;22:78-90.

63. Stackowicz J, Gaudenzio N, Serhan N, Conde E, Godon O, Marichal T, et al. Neutrophil-specific gain-of-function mutations in Nlrp3 promote development of

cryopyrin-associated periodic syndrome. J Exp Med 2021;218.

64. Sawant KV, Sepuru KM, Lowry E, Penaranda B, Frevert CW, Garofalo RP, et al. Neutrophil recruitment by chemokines Cxcl1/KC and Cxcl2/MIP2: Role of Cxcr2 activation and glycosaminoglycan interactions. J Leukoc Biol 2021;109:777-91.

65. Girbl T, Lenn T, Perez L, Rolas L, Barkaway A, Thiriot A, et al. Distinct Compartmentalization of the Chemokines CXCL1 and CXCL2 and the Atypical Receptor ACKR1 Determine Discrete Stages of Neutrophil Diapedesis. Immunity 2018;49:1062-76.e6.

66. Aryal R, Patabendige A. Blood-brain barrier disruption in atrial fibrillation: a potential contributor to the increased risk of dementia and worsening of stroke outcomes? Open Biol 2021;11:200396.

67. Daneman R, Rescigno M. The gut immune barrier and the blood-brain barrier: are they so different? Immunity 2009;31:722-35.

68. Park HJ, Shin JY, Kim HN, Oh SH, Song SK, Lee PH. Mesenchymal stem cells stabilize the blood-brain barrier through regulation of astrocytes. Stem Cell Res Ther 2015;6:187.

69. Wang P, Ren Q, Shi M, Liu Y, Bai H, Chang YZ. Overexpression of Mitochondrial Ferritin Enhances Blood-Brain Barrier Integrity Following Ischemic Stroke in Mice by Maintaining Iron Homeostasis in Endothelial Cells. Antioxidants (Basel) 2022;11.

70. Jin X, Riew TR, Kim S, Kim HL, Lee MY. Spatiotemporal Profile and Morphological Changes of NG2 Glia in the CA1 Region of the Rat Hippocampus after Transient Forebrain Ischemia. Exp Neurobiol 2020;29:50-69.

71. Kaushik DK, Bhattacharya A, Lozinski BM, Wee Yong V. Pericytes as mediators of infiltration of macrophages in multiple sclerosis. J Neuroinflammation 2021;18:301.

72. Herz J, Sabellek P, Lane TE, Gunzer M, Hermann DM, Doeppner TR. Role of Neutrophils in Exacerbation of Brain Injury After Focal Cerebral Ischemia in Hyperlipidemic Mice. Stroke 2015;46:2916-25.

73. Papayannopoulos V. Neutrophil extracellular traps in immunity and disease. Nat Rev Immunol 2018;18:134-47.

74. Lee KH, Kronbichler A, Park DD, Park Y, Moon H, Kim H, et al. Neutrophil extracellular traps (NETs) in autoimmune diseases: A comprehensive review. Autoimmun Rev 2017;16:1160-73.

75. Kienhöfer D, Hahn J, Stoof J, Csepregi JZ, Reinwald C, Urbonaviciute V, et al. Experimental lupus is aggravated in mouse strains with impaired induction of neutrophil extracellular traps. JCI Insight 2017;2.

76. Tillack K, Naegele M, Haueis C, Schippling S, Wandinger KP, Martin R, et al. Gender differences in circulating levels of neutrophil extracellular traps in serum of multiple sclerosis patients. J Neuroimmunol 2013;261:108-19.

77. Grilz E, Mauracher LM, Posch F, Königsbrügge O, Zöchbauer-Müller S, Marosi

C, et al. Citrullinated histone H3, a biomarker for neutrophil extracellular trap formation, predicts the risk of mortality in patients with cancer. Br J Haematol 2019;186:311-20.

78. Kim SW, Lee H, Lee HK, Kim ID, Lee JK. Neutrophil extracellular trap induced by HMGB1 exacerbates damages in the ischemic brain. Acta Neuropathol Commun 2019;7:94.

79. Campos J, Ponomaryov T, De Prendergast A, Whitworth K, Smith CW, Khan AO, et al. Neutrophil extracellular traps and inflammasomes cooperatively promote venous thrombosis in mice. Blood Adv 2021;5:2319-24.

80. Vaibhav K, Braun M, Alverson K, Khodadadi H, Kutiyanawalla A, Ward A, et al. Neutrophil extracellular traps exacerbate neurological deficits after traumatic brain injury. Sci Adv 2020;6:eaax8847.

81. Pedersen F, Waschki B, Marwitz S, Goldmann T, Kirsten A, Malmgren A, et al. Neutrophil extracellular trap formation is regulated by CXCR2 in COPD neutrophils. Eur Respir J 2018;51.

82. Rodrigues DAS, Prestes EB, Gama AMS, Silva LS, Pinheiro AAS, Ribeiro JMC, et al. CXCR4 and MIF are required for neutrophil extracellular trap release triggered by Plasmodium-infected erythrocytes. PLoS Pathog 2020;16:e1008230.

83. Yan Z, Yang W, Parkitny L, Gibson SA, Lee KS, Collins F, et al. Deficiency of Socs3 leads to brain-targeted EAE via enhanced neutrophil activation and ROS production. JCI Insight 2019;5.

84. Gierlikowska B, Stachura A, Gierlikowski W, Demkow U. Phagocytosis, Degranulation and Extracellular Traps Release by Neutrophils-The Current Knowledge, Pharmacological Modulation and Future Prospects. Front Pharmacol 2021;12:666732.

85. Martín-Martín B, Nabokina SM, Blasi J, Lazo PA, Mollinedo F. Involvement of SNAP-23 and syntaxin 6 in human neutrophil exocytosis. Blood 2000;96:2574-83.

86. Miralda I, Uriarte SM, McLeish KR. Multiple Phenotypic Changes Define Neutrophil Priming. Front Cell Infect Microbiol 2017;7:217.

87. Noubade R, Wong K, Ota N, Rutz S, Eidenschenk C, Valdez PA, et al. NRROS negatively regulates reactive oxygen species during host defence and autoimmunity. Nature 2014;509:235-9.

88. Broggi A, Tan Y, Granucci F, Zanoni I. IFN-λ suppresses intestinal inflammation by non-translational regulation of neutrophil function. Nat Immunol 2017;18:1084-93.

89. Azzouz D, Khan MA, Palaniyar N. ROS induces NETosis by oxidizing DNA and initiating DNA repair. Cell Death Discov 2021;7:113.

90. Rohrbach AS, Slade DJ, Thompson PR, Mowen KA. Activation of PAD4 in NET formation. Front Immunol 2012;3:360.

91. Castanheira FVS, Kubes P. Neutrophils and NETs in modulating acute and chronic inflammation. Blood 2019;133:2178-85.

92. Poli V, Zanoni I. Neutrophil intrinsic and extrinsic regulation of NETosis in health and disease. Trends Microbiol 2023;31:280-93.

93. Ou Q, Fang JQ, Zhang ZS, Chi Z, Fang J, Xu DY, et al. TcpC inhibits neutrophil extracellular trap formation by enhancing ubiquitination mediated degradation of peptidylarginine deiminase 4. Nat Commun 2021;12:3481.

94. Constantinescu CS, Farooqi N, O'Brien K, Gran B. Experimental autoimmune encephalomyelitis (EAE) as a model for multiple sclerosis (MS). Br J Pharmacol 2011;164:1079-106.

95. Ma Q, Chen S, Hu Q, Feng H, Zhang JH, Tang J. NLRP3 inflammasome contributes to inflammation after intracerebral hemorrhage. Ann Neurol 2014;75:209-19.

96. Guo Z, Yu S, Chen X, Zheng P, Hu T, Duan Z, et al. Suppression of NLRP3 attenuates hemorrhagic transformation after delayed rtPA treatment in thromboembolic stroke rats: Involvement of neutrophil recruitment. Brain Res Bull 2018;137:229-40.

97. Palomino-Antolin A, Narros-Fernández P, Farré-Alins V, Sevilla-Montero J, Decouty-Pérez C, Lopez-Rodriguez AB, et al. Time-dependent dual effect of NLRP3 inflammasome in brain ischaemia. Br J Pharmacol 2022;179:1395-410.

98. Bellut M, Papp L, Bieber M, Kraft P, Stoll G, Schuhmann MK. NLPR3 inflammasome inhibition alleviates hypoxic endothelial cell death in vitro and protects blood-brain barrier integrity in murine stroke. Cell Death Dis

2021;13:20.

99. Yao HW, Kuan CY. Early neutrophil infiltration is critical for inflammation-sensitized hypoxic-ischemic brain injury in newborns. J Cereb Blood Flow Metab 2020;40:2188-200.

100. Wedmore CV, Williams TJ. Control of vascular permeability by polymorphonuclear leukocytes in inflammation. Nature 1981;289:646-50.

101. Tinsley JH, Wu MH, Ma W, Taulman AC, Yuan SY. Activated neutrophils induce hyperpermeability and phosphorylation of adherens junction proteins in coronary venular endothelial cells. J Biol Chem 1999;274:24930-4.

102. Wang Q, Doerschuk CM. The signaling pathways induced by neutrophil-endothelial cell adhesion. Antioxid Redox Signal 2002;4:39-47.

103. Moxon-Emre I, Schlichter LC. Neutrophil depletion reduces blood-brain barrier breakdown, axon injury, and inflammation after intracerebral hemorrhage. J Neuropathol Exp Neurol 2011;70:218-35.

104. Cambier S, Gouwy M, Proost P. The chemokines CXCL8 and CXCL12: molecular and functional properties, role in disease and efforts towards pharmacological intervention. Cell Mol Immunol 2023;20:217-51.

105. Hughes CE, Nibbs RJB. A guide to chemokines and their receptors. Febs j 2018;285:2944-71.

106. Haarmann A, Schuhmann MK, Silwedel C, Monoranu CM, Stoll G, Buttmann M. Human Brain Endothelial CXCR2 is Inflammation-Inducible and Mediates

CXCL5- and CXCL8-Triggered Paraendothelial Barrier Breakdown. Int J Mol Sci 2019;20.

107. Yu H, Huang X, Ma Y, Gao M, Wang O, Gao T, et al. Interleukin-8 regulates endothelial permeability by down-regulation of tight junction but not dependent on integrins induced focal adhesions. Int J Biol Sci 2013;9:966-79.

108. Lo U, Selvaraj V, Plane JM, Chechneva OV, Otsu K, Deng W. p38α (MAPK14) critically regulates the immunological response and the production of specific cytokines and chemokines in astrocytes. Sci Rep 2014;4:7405.

109. Wu F, Zhao Y, Jiao T, Shi D, Zhu X, Zhang M, et al. CXCR2 is essential for cerebral endothelial activation and leukocyte recruitment during neuroinflammation. J Neuroinflammation 2015;12:98.

110. Guijarro-Muñoz I, Compte M, Álvarez-Cienfuegos A, Álvarez-Vallina L, Sanz L. Lipopolysaccharide activates Toll-like receptor 4 (TLR4)-mediated NF-κB signaling pathway and proinflammatory response in human pericytes. J Biol Chem 2014;289:2457-68.

111. Lentini G, De Gaetano GV, Famà A, Galbo R, Coppolino F, Mancuso G, et al. Neutrophils discriminate live from dead bacteria by integrating signals initiated by Fprs and TLRs. Embo j 2022;41:e109386.

112. Mei HX, Ye Y, Xu HR, Xiang SY, Yang Q, Ma HY, et al. LXA4 Inhibits Lipopolysaccharide-Induced Inflammatory Cell Accumulation by Resident Macrophages in Mice. J Inflamm Res 2021;14:1375-85.

113. Chen Z, Hu W, Mendez MJ, Gossman ZC, Chomyk A, Boylan BT, et al. Neuroprotection by Preconditioning in Mice is Dependent on MyD88-Mediated CXCL10 Expression in Endothelial Cells. ASN Neuro 2023;15:17590914221146365.

114. Wu F, Chen X, Zhai L, Wang H, Sun M, Song C, et al. CXCR2 antagonist attenuates neutrophil transmigration into brain in a murine model of LPS induced neuroinflammation. Biochem Biophys Res Commun 2020;529:839-45.

115. Zhou H, Andonegui G, Wong CH, Kubes P. Role of endothelial TLR4 for neutrophil recruitment into central nervous system microvessels in systemic inflammation. J Immunol 2009;183:5244-50.

116. He H, Geng T, Chen P, Wang M, Hu J, Kang L, et al. NK cells promote neutrophil recruitment in the brain during sepsis-induced neuroinflammation. Sci Rep 2016;6:27711.

117. Coffelt SB, Wellenstein MD, de Visser KE. Neutrophils in cancer: neutral no more. Nat Rev Cancer 2016;16:431-46.

118. Yi L, Ju Y, He Y, Yin X, Xu Y, Weng T. Intraperitoneal injection of Desferal® alleviated the age-related bone loss and senescence of bone marrow stromal cells in rats. Stem Cell Res Ther 2021;12:45.

119. Kadry H, Noorani B, Cucullo L. A blood-brain barrier overview on structure, function, impairment, and biomarkers of integrity. Fluids Barriers CNS 2020;17:69.

120. Echchannaoui H, Frei K, Letiembre M, Strieter RM, Adachi Y, Landmann R. CD14 deficiency leads to increased MIP-2 production, CXCR2 expression, neutrophil transmigration, and early death in pneumococcal infection. J Leukoc Biol 2005;78:705-15.

121. Cao T, Yuan X, Fang H, Chen J, Xue K, Li Z, et al. Neutrophil extracellular traps promote keratinocyte inflammation via AIM2 inflammasome and AIM2-XIAP in psoriasis. Exp Dermatol 2023;32:368-78.

122. Bhardwaj A, Sapra L, Saini C, Azam Z, Mishra PK, Verma B, et al. COVID-19: Immunology, Immunopathogenesis and Potential Therapies. Int Rev Immunol 2022;41:171-206.

123. Tall AR, Westerterp M. Inflammasomes, neutrophil extracellular traps, and cholesterol. J Lipid Res 2019;60:721-7.

124. Peoples JN, Saraf A, Ghazal N, Pham TT, Kwong JQ. Mitochondrial dysfunction and oxidative stress in heart disease. Exp Mol Med 2019;51:1-13.

125. Hyun YM, Hong CW. Deep insight into neutrophil trafficking in various organs. J Leukoc Biol 2017;102:617-29.

126. Park SA, Hyun YM. Neutrophil Extravasation Cascade: What Can We Learn from Two-photon Intravital Imaging? Immune Netw 2016;16:317-21.

127. Zen K, Guo YL, Li LM, Bian Z, Zhang CY, Liu Y. Cleavage of the CD11b extracellular domain by the leukocyte serprocidins is critical for neutrophil detachment during chemotaxis. Blood 2011;117:4885-94.

128. Loos J, Schmaul S, Noll TM, Paterka M, Schillner M, Löffel JT, et al. Functional characteristics of Th1, Th17, and ex-Th17 cells in EAE revealed by intravital two-photon microscopy. J Neuroinflammation 2020;17:357.

129. Xiong Y, Wu X, Qu X, Xie X, Ren Y. Functions of T-cell subsets and their related cytokines in the pathological processes of autoimmune encephalomyelitic mice. Int J Clin Exp Pathol 2018;11:4817-26.

130. Wilson AS, Randall KL, Pettitt JA, Ellyard JI, Blumenthal A, Enders A, et al. Neutrophil extracellular traps and their histones promote Th17 cell differentiation directly via TLR2. Nat Commun 2022;13:528.

131. Lambert S, Hambro CA, Johnston A, Stuart PE, Tsoi LC, Nair RP, et al. Neutrophil Extracellular Traps Induce Human Th17 Cells: Effect of Psoriasis-Associated TRAF3IP2 Genotype. J Invest Dermatol 2019;139:1245-53.

132. Yousefi S, Simon D, Stojkov D, Karsonova A, Karaulov A, Simon HU. In vivo evidence for extracellular DNA trap formation. Cell Death Dis 2020;11:300.

133. Huang SU, O'Sullivan KM. The Expanding Role of Extracellular Traps in Inflammation and Autoimmunity: The New Players in Casting Dark Webs. Int J Mol Sci 2022;23.

134. Pierson ER, Wagner CA, Goverman JM. The contribution of neutrophils to CNS autoimmunity. Clin Immunol 2018;189:23-8.

135. Carlson T, Kroenke M, Rao P, Lane TE, Segal B. The Th17-ELR+ CXC chemokine pathway is essential for the development of central nervous system

autoimmune disease. J Exp Med 2008;205:811-23.

136. Aubé B, Lévesque SA, Paré A, Chamma É, Kébir H, Gorina R, et al. Neutrophils mediate blood-spinal cord barrier disruption in demyelinating neuroinflammatory diseases. J Immunol 2014;193:2438-54.

137. Allen C, Thornton P, Denes A, McColl BW, Pierozynski A, Monestier M, et al. Neutrophil cerebrovascular transmigration triggers rapid neurotoxicity through release of proteases associated with decondensed DNA. J Immunol 2012;189:381-92.

138. Karni A, Koldzic DN, Bharanidharan P, Khoury SJ, Weiner HL. IL-18 is linked to raised IFN-gamma in multiple sclerosis and is induced by activated CD4(+) T cells via CD40-CD40 ligand interactions. J Neuroimmunol 2002;125:134-40.

139. Shi FD, Takeda K, Akira S, Sarvetnick N, Ljunggren HG. IL-18 directs autoreactive T cells and promotes autodestruction in the central nervous system via induction of IFN-gamma by NK cells. J Immunol 2000;165:3099-104.

140. Yu S, Chen Z, Mix E, Zhu SW, Winblad B, Ljunggren HG, et al. Neutralizing antibodies to IL-18 ameliorate experimental autoimmune neuritis by counter-regulation of autoreactive Th1 responses to peripheral myelin antigen. J Neuropathol Exp Neurol 2002;61:614-22.

141. Pierson E, Simmons SB, Castelli L, Goverman JM. Mechanisms regulating regional localization of inflammation during CNS autoimmunity. Immunol Rev 2012;248:205-15.

Abstract in Korean

마우스 뇌 내 BBB 투과도 및 호중구 기능 조절에 의한 NLRP3의 EAE 중증도 악화 효과

호중구 침윤 및 호중구 세포외 덫 (NETs)은 다발성 경화증 (MS) 및 실험적 자가면역 뇌척수염 (EAE)을 포함한 여러 뇌 질환의 병리에서 중요한 역할을 하는 것으로 알려져 있다. 선행 연구에 의하면 세포 내 센서 분자인 NLRP3 가 염증이 있는 뇌에서 호중구의 기능과 이동성에 영향을 미칠 수 있음이 보고된 바 있다. 그러나 NLRP3 염증복합체가 뇌로의 호중구 침윤 과정에서 작용하는 구체적인 분자 기전은 거의 알려져 있지 않다. 뿐만 아니라 여러 연구에 의해 NLRP3 의 부재가 EAE 의 중증도를 완화시킬 수 있음이 확인되었지만, NLRP3 가 EAE 병인에 미치는 역할과 NET 형성에 대한 기전에 관해 아직 완전히 이해되지 않았다. 본 연구의 결과, 호중구가 NLRP3 발현을 통해 초기 신경염증에 기여하는 것이 관측되었으며 NLRP3 는 호중구 초기 활성화에는 필요하지 않지만, 호중구 침윤에는 필수적인 것 또한 관측되었다. 특히, 호중구에서의 NLRP3 활성화는 CXCL1 과 CXCL2 발현을 증가시켜 CXCR2 의존적인 BBB 손상과 뇌조직으로의 호중구 침윤을 유도했다.

또한, 염증이 있는 뇌에서 성상세포, 혈관주위세포, 호중구 및 내피세포에 의해 생성된 CXCL1 과 CXCL2 는 뇌 내피세포에서 BBB 투과성을 조절하는 결합 단백질인 claudin-5 의 발현을 직접적으로 감소시킬 수 있음을 확인했다. EAE 모델을 활용한 본 연구의 결과에선, EAE 병인 동안 호중구가 중추신경계로 침윤 및 NETs 를 형성하고, 생성된 NETs 는 뇌조직내 축적된다는 것이 관측되었다. 추가적으로, NLRP3 는 주로 뇌에서 NET 형성을 촉진하여 Th1 및 Th17 세포의 중추신경계로의 유입을 촉진하고 탈 수초화를 유도함으로써 EAE 의 중증도를 악화시킴을 확인했다. 이 연구는 NLRP3 가 호중구의 이동 패턴과 기능적 표현형을 조절하여 뇌 조직에서의 침윤과 ROS-의존적인 NET 형성을 촉진한다는 증거를 제공한다. 결과적으로, NLRP3 를 억제하는 것은 BBB 손상, 호중구 침윤 및 뇌에서의 NET 형성을 줄여 EAE 의 중증도를 완화시키는 치료 전략으로 고려될 수 있음을 시사한다.

핵심되는 말 : 호중구, 호중구 세포외 덫 (NETs), 다발성 경화증, 실험적 자가면역 뇌 척수염 (EAE), NLRP3, 중추 신경계, CXCR2, 혈액뇌장벽, 탈 수초화

PUBLICATION LIST

1. Byun DJ*, **Lee J***, Ko K, Hyun YM. NLRP3 exacerbates EAE severity through ROS-dependent NET formation in the mouse brain. Cell Commun Signal. 2024 Feb 2;22(1):96.